2013

THE ROLE OF MUSCLE-SYNTHESIZED BRAIN-DERIVED NEUROTROPHIC FACTOR (BDNF) IN THE HEALTH AND MAINTENANCE OF MOTORNEURONS

Emily J. Pomeroy
Northern Michigan University

THE ROLE OF MUSCLE-SYNTHESIZED BRAIN-DERIVED NEUROTROPHIC FACTOR (BDNF) IN THE HEALTH AND MAINTENANCE OF MOTORNEURONS

By

Emily J. Pomeroy

THESIS

Submitted
To
Northern Michigan
University
In partial fulfillment of the
Requirements
For the degree
Of

MASTER OF SCIENCE

Office of Graduate Education and Research

2013

SIGNATURE APPROVAL FORM

Title of Thesis:

The Role of Muscle-Synthesized Brain-Derived Neurotrophic Factor (BDNF) in the Health and Maintenance of Motorneurons

This thesis by Emily J. Pomeroy is recommended for approval by the student's Thesis Committee and Department Head in the Department of Biology and by the Assistant Provost of Graduate Education and Research.

_____

Committee Chair: Dr. Erich Ottem Date

_____

First Reader: Dr. Robert Belton Date

_____

Second Reader: Dr. Adam Prus Date

_____

Third Reader: Dr. Robert Winn Date

_____

Department Head: Dr. John Rebers Date

_____

Dr. Brian D. Cherry Date
Assistant Provost of Graduate Education and Research

ABSTRACT

Neuromuscular diseases are characterized by degeneration of motorneurons and atrophy of the muscles which they innervate. At the cellular level, neuropathological markers include a decrease in cell body size, dendritic atrophy, loss of synaptic input, and vacuolation. These markers are precursors to eventual apoptotic death of neurons. Although the progressive pathological hallmarks of most neuromuscular diseases are well-characterized, their origins, in many cases, remain largely unknown. One possible trigger of pathology associated with neuromuscular diseases is a loss or reduction of brain-derived neurotrophic factor (BDNF) in the motor unit. BDNF is a neurotrophic protein synthesized by both motorneurons and muscles, and promotes cell survival, growth and differentiation. Preliminary data indicate that mice lacking (or with reduced) BDNF synthesized by skeletal muscles display neuromuscular deficits in adulthood, including decreased grip strength, decreased stride length, and increased clasping behavior. We hypothesized that absent or reduced BDNF synthesized by muscles will lead to many of the same neuropathological markers present in common neuromuscular diseases. To address this possibility, we used a Cre-recombinase/LoxP gene knockout system to generate experimental mice missing one or both alleles of the BDNF gene only in skeletal muscle. To assess transgenic mice for progressive neuropathological markers, Nissl staining, immunocytochemistry, and light and confocal microscopy were utilized. These techniques allowed us to identify and characterize potential pathological changes in motorneurons and associated. This thesis will focus on progressive pathology associated with spinal motorneurons. Motorneurons of experimental and control mice were enumerated and analyzed for BDNF expression, dendritic atrophy, loss of synaptic input, and the appearance of cellular vacuolation. Analysis was carried out using two age groups (30 d and 120 d) to determine whether the appearance of potential cellular pathology was progressive. Results indicate that reduced or absent muscle-synthesized BDNF leads to decreased cell body size, altered amounts of BDNF protein present in motorneurons, and decreased length and diameter of motorneuron dendrites. This phenotype is similar to neuropathy seen in neuromuscular diseases.

ACKNOWLEDGEMENTS

This research was made possible by financial support from Grant R15 NS074367-01A1 to E.N.O. from the National Institute of Neurological Disorders and Stroke (of the National Institutes of Health) and the Northern Michigan University Excellence in Education Grant.

I extend my utter gratitude to my graduate adviser and mentor, Erich N. Ottem, for nearly four years of continued direction and support. Additionally, I thank the members of my graduate committee, Dr. Robert Belton, Dr. Adam Prus, and Dr. Robert Winn for their guidance; Dr. Alan Rebertus for assistance with statistical analysis; Jason Moody for IT support; and the members of the Ottem Laboratory for their hard work and contribution, especially Kate Abrahamsson, Ryan Budin, Calvin Fries, and Leah Schuman.

Finally, I am grateful for the unending love, support, and assistance from my parents: Joy and Russell Pomeroy, my sister: Rachel Pomeroy, and my boyfriend: Jason Moody throughout my graduate career.

TABLE OF CONTENTS

LIST OF TABLES AND FIGURES

CHAPTER ONE: INTRODUCTION & LITERATURE REVIEW

Neurotrophins, also known as neurotrophic factors, are a family of diffusible proteins that generally promote the survival, growth, and differentiation of neurons [1]. The neurotrophin family includes nerve growth factor (NGF), neurotrophin-3 (NT-3), neurotrophin-4 (NT-4), neurotrophin-5 (NT-5) and brain-derived neurotrophic factor (BDNF), among others. Neurotrophic factors are important for the growth of developing neurons and the maintenance of mature neurons throughout the central and peripheral nervous systems [1-3]. At times during development, they can play an opposite role, and function to prune unwanted neurons from the nervous system [4-7]. Neurotrophins function as anterograde, retrograde, autocrine, and paracrine signaling molecules. Anterograde transport (cell body to axon terminal) and retrograde transport (axon terminal to cell body) are neuron-specific systems for transporting cargo. The mechanisms of these systems are described in detail later in this introduction. As such, they are released from both presynaptic terminals and postsynaptic membranes and bind to receptors expressed by target cells (anterograde, retrograde, paracrine) or the cell that released them (autocrine). NGF, NT 3-5, and BDNF bind to two families of receptors – (1) $p75^{NTR}$, which binds all five neurotrophins, and (2) the tyrosine kinase (Trk) receptors TrkA, TrkB, and TrkC, which have differing binding affinities for each neurotrophin [8]. BDNF, the focus of this project, preferentially binds to the TrkB receptor.

Due to their involvement in regulating cell survival and apoptosis, neurotrophic factors have been well-characterized in models of nervous system development. More recently, their roles in the postnatal and adult maintenance of functional neural morphology and synaptic plasticity have been described [9-13]. In particular, BDNF has been shown to play a role in

synaptic plasticity and memory formation in both the hippocampus and the amygdala [12, 14-17]. Fear-conditioning in rats leads to upregulation of BDNF, which aids in the consolidation of fear memory in the amygdala [14, 15]. Application of antagonists for the TrkB receptor impaired consolidation of fear learning and extinction retention [15-17]. BDNF also modulates long-term potentiation (LTP) in the adult hippocampus. Within the hippocampus, BDNF is stored in dendritic processes and is released after high frequency stimulation (HFS) [18]. The TrkB receptor is located both pre- and postsynaptically [19]. This distribution indicates that BDNF can initiate a signaling cascade in both an anterograde and a retrograde manner. A review by Bramham and Messodusi (2005) describes the permissive and instructive roles played by BDNF in hippocampal synaptic plasticity. The permissive role refers to maintenance of the synapse by basal levels of BDNF (not released due to HFS). The instructive refers to the action of HFS-evoked BDNF release. In this situation, BDNF activates pathways leading to local enhanced translation of synaptic-associated mRNA stored in dendrites and is implicated in the process of long-term potentiation (LTP) in memory formation [20-23]. Additionally, BDNF signaling leads to enhanced actin polymerization in dendritic spines, thus increasing the number and size of synapses as a result of HFS. This actin polymerization was diminished by a BDNF antagonist [24]. In addition to the neurotrophin's role in hippocampal and amygdalar function, the distribution of BDNF and its receptor is observed throughout the CNS, including the spinal cord, thus suggesting a widespread role for the protein [46].

As indicated, BDNF and TrkB proteins are expressed by multiple neural phenotypes in the telencephalon, diencephalon, midbrain, brainstem, and spinal cord. In addition, these proteins can be found in the peripheral nervous system, as well as many other tissues, including liver, kidneys, retina, prostate, and skeletal muscle [25-28]. Recent research suggests that it is

retrograde signaling of the neurotrophins (from postsynaptic cell to presynaptic cell) in particular that plays a significant role in the maintenance, growth, and synaptic plasticity of the innervating neuron [8, 29-31]. This is of particular interest in research involving the spinal motor units, as skeletal muscle has been shown to be a significant source of neurotrophin synthesis during development [1-3, 32]. Recent studies reveal BDNF as one of the key players in a trophic support system that maintains the motorneurons and muscles of a motor unit in adulthood [33-35]. Neurotrophic-dependent maintenance of an adult neuromuscular system is typified by the well-described spinal nucleus of the bulbocavernosus (SNB) in rodents. The SNB is a sexually dimorphic nucleus of the lumbar spinal cord that is significantly larger in males, as it innervates the bulbocavernosus and levator ani muscles of the penis, as well as the external anal sphincter. Treatment of severed SNB axons with BDNF can prevent both axotomy- or castration-induced declines in soma size and expression of androgen receptor (AR) of SNB motorneurons [36-38]. Additionally, treatment of axotomized male rats with BDNF and testosterone will ameliorate axotomy-associated declines in dendritic arborizations [36, 39]. These studies show that androgens upregulate TrkB receptors expressed by SNB motorneurons which are believed to retrogradely transport muscle-synthesized BDNF to the cell body. A group of researchers also recently described the synergistic, trophic effects of androgens and BDNF in the quadriceps muscles and their innervating motorneurons – a non-sexually dimorphic neuromuscular system. In their study, castration reduced immunolabeling of BDNF protein in quadriceps muscles and motorneurons, and treatment with testosterone ameliorated this deficit [40, 41]. In another non-dimorphic system involving spinal cord injury rather than axotomy, increased BDNF, along with glial-derived neurotrophic factor (GDNF), in exercised muscles was found to ameliorate the atrophy of muscle and motorneurons, and improve pain, in rats with spinal cord injury [42, 43].

This retrograde transport provides trophic support, maintaining soma size and dendritic arborization. Recent findings also suggest that BDNF can activate different signal transduction cascades which may elicit different cellular responses, depending on the source of the neurotrophin. In the hippocampus, for example, target-derived retrograde BDNF activates PI3K/Akt pathway, while other sources activate the MEK/ERK pathway [44]. The PI3K/Akt pathway, when activated by BDNF, has been shown to cause an enlargement of post-synaptic density protein 95 (PSD-95), a protein associated with the strengthening of synapses [45]. A recent review describes that target-derived BDNF activated the PI3/Akt pathway to initiate both transcriptional-dependent and independent pathways that promote cell survival [46]. Conversely, activation of the MEK/ERK pathway by BDNF has been implicated protection against the excitotoxic effects of glutamate activity [47, 48].

It should be noted that the BDNF gene is comprised of eight non-coding exons (I-VIII), and one coding exon (IX). During transcription, all but one non-coding exon are spliced out, and the remaining non-coding exon is involved in trafficking the mRNA to various cellular compartments (Figure 1) [49, 50]. Thus, within a cell, non-coding exons can dictate the precise role that BDNF will play due to differential trafficking. In some cases, BDNF will be trafficked to dendrites and play a role in maintaining dendritic and synaptic structure; in other cases, BDNF will be transported to presynaptic terminals and act as an anterograde neurotransmitter [51, 52]. Several promoters and repressors have been described which help to determine which non-coding exon will be expressed. A recent study describes differential expression of the non-coding exons in various neural and non-neural tissues in both mice and rats [53]. This differential expression suggests BDNF localization and function can differ depending on the tissue in which it is synthesized.

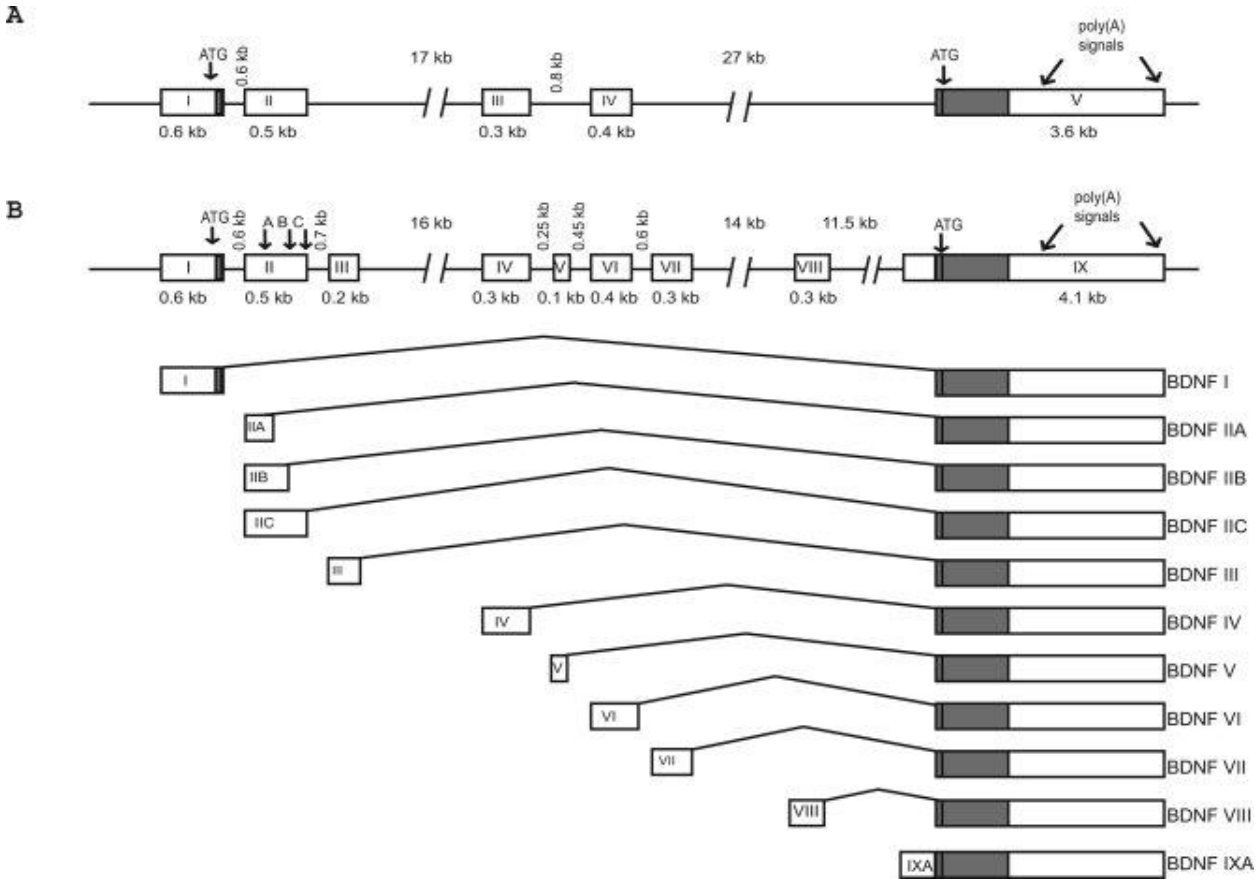

Figure 1, from Aid et al. (2007). Exon/intron structure and alternative transcripts of mouse and rat BDNF genes. **A:** Rat BDNF gene structure as described by Timmusk et al. (1993). Exons are shown as boxes and introns are shown as lines. **B:** The new arrangement of exons and introns of mouse and rat BDNF genes as determined by analyzing genomic and mRNA sequence data using bioinformatics, 5′ RACE, and RT-PCR. The schematic representation of BDNF transcripts in relation to the gene is shown below the gene structure. Protein coding regions are shown as solid boxes and untranslated regions are shown as open boxes. Each of the eight 5′ untranslated exons is spliced to the common 3′ protein coding exon IX. In addition, transcription can be initiated in the intron before the protein coding exon, which results in IXA transcripts containing 5′ extended coding exon. Each transcription unit may use one of the two alternative polyadenylation signals in the 3′ exon (arrows). For exon II, three different transcript variants, IIA, IIB, and IIC, are generated as a result of using alternative splice-donor sites in exon II (arrows marked A, B, and C) [53].

BDNF synthesis by skeletal muscle is variable, and the specific mechanisms of regulation of expression of the neurotrophin by muscle fibers under normal conditions are unclear. Some studies show that BDNF is present in muscle fibers during development and in adult mice and birds [2]. Others report that BDNF is present only in adult muscle fibers, and absent during

development [1, 54]. The expression of BDNF by skeletal muscle can be altered by varying physical and pathological conditions. For example, recent findings show that exercise (i.e., skeletal muscle contraction) leads to an increase in BDNF mRNA and protein levels in skeletal muscle [55-57]. In rats, after 5 days of treadmill exercise, BDNF mRNA was significantly increased in the soleus muscle, and not in innervating motorneurons. Interestingly, there was no significant increase in BDNF protein levels in the soleus muscle, but the levels of BDNF mRNA were significantly higher. The presence of mRNA suggests that BDNF is being synthesized by muscles, then exported to motorneurons [58]. A subsequent study by the same authors demonstrated a differential time course of BDNF and TrkB expression in muscle and spinal cord after exercise in rats. BDNF expression increased in soleus muscles after three days of exercise, and began to decrease at day seven. Conversely, BDNF expression continued to increase at day seven in the spinal cord. These authors also determined whether exercise influenced the expression of downstream effectors of BDNF signaling that are involved in synaptic maintenance and plasticity, including synapsin I, growth-associated protein 43 (GAP-43) and cyclic AMP response element-binding protein (CREB). All downstream effectors of BDNF-TrkB signaling were increased in the spinal cord of exercised rats. In addition, synapsin I was initially elevated in the soleus muscle, but declined to control levels after seven days of exercise [59]. These results suggest that BDNF was produced by stimulated, contracting skeletal muscles and was likely transported retrogradely to innervating motorneurons to affect physiological functioning. In summary, BDNF signaling to responsive cells is complex and multi-directional. Motorneurons are supplied with BDNF from several sources. The neurotrophin is synthesized by motorneurons, and is also endocytosed from postsynaptic targets [60]. As described in the next section, it is hypothesized that BDNF produced in adult target cells, such as skeletal muscle,

acts retrogradely to strengthen and potentiate the presynaptic neuron. In the case of neuromuscular systems, skeletal muscle fibers would therefore provide BDNF to regulate the growth and morphological maintenance of innervating motorneurons [61, 62].

The hypothesis that muscle-synthesized BDNF is transported retrogradely to innervating motorneurons requires a detailed discussion of this mechanism. Motorneurons may be up to one meter in length and require specific transport processes to move proteins and other molecules efficiently to and from the soma in the ventral horns of the spinal cord. The terms anterograde and retrograde transport refer to neuron-specific systems that allow movement of material from cell body to axon and from axon to cell body, respectively. This is made possible by cytoskeletal microtubules which run the length of the axon and serve as tracks for transportation. Motor proteins move along the microtubules with bound cargo including organelles, proteins, and vesicles of mRNA [63]. The motor proteins include members of the kinesin and dynein families. Kinesins are two-headed, ATP-driven proteins that move along the microtubules in 8 nm steps, and are generally associated with anterograde transport [64]. Dynein proteins are massive multisubunit complexes that are associated with the protein dynactin, which allows for transport of cargo retrogradely along the microtubules [65]. This extensively-studied transport system makes it plausible for muscle-synthesized neurotrophic factors, such as BDNF, to retrogradely support motorneurons. Hypothetically, when a motorneuron signals to a muscle fiber to contract, the muscle responds by contracting and releasing BDNF. After being released from the muscle cell at the neuromuscular junction (NMJ), BDNF binds to its TrkB receptor on the motorneuron. Ligand binding induces dimerization of the receptor, which is then internalized and transported retrogradely via the dynein complex proteins to the soma. Here, the signal transduction cascades initialized by BDNF-TrkB complexes leads to differential gene transcription [8, 66-68]. In the

motorneuron, it is hypothesized that BDNF acts as a positive feedback signal increasing the size and strength of the synapses formed between the motorneurons and the neurons of the motor cortex, which initiated the original muscle contraction [58, 60, 69, 70]. This feedback system could be disrupted in diseases which affect the size, health, and efficacy of muscle fibers.

Indeed, BDNF and other neurotrophic factors have been implicated in many neuromuscular disease processes. A loss or reduction of neurotrophic factors isn't necessarily the underlying cause of such disorders, but it could be a downstream effect of atrophy of the motor unit. Of particular interest are motor neuron diseases (MNDs), including amyotrophic lateral sclerosis (ALS). This is because unlike many predictably progressing neuromuscular diseases, such as Huntington's chorea, Duchenne's muscular dystrophy, or spinal muscular atrophy, the onset of ALS and other MNDs cannot always be traced to a malfunction of a protein or mutation of a single gene. Research focused on MNDs has brought to light many different environmental, cellular, and genetic factors that can increase susceptibility to pathology. Among these are exposure to heavy metals, excessive glutamate stimulation (excitotoxicity), oxidative stress, mitochondrial dysfunction, impaired axonal transport, aggregation of cellular proteins – specifically neurofilaments, and deficits in neurotrophic factors [2, 3, 58, 71]. These different pathways all lead to the same pathological hallmarks of disease. Thus, MNDs are diseases defined by a common outcome, rather than a common cause.

Most forms of ALS, in particular, are characterized by degeneration of motorneurons and atrophy of the muscles which they innervate [72, 73]. The neural and muscular pathology causes ALS patients to suffer from a loss of motor function that eventually leads to paralysis. In most cases, initial muscle atrophy occurs in the appendages, which causes a loss of function in the extremities. As the disease progresses, the axial muscles are affected. When axial muscles

such as the diaphragm and intercostals muscles fail, the patient can no longer breathe without ventilatory support [73-76]. The specific neuronal pathology of such diseases includes an overall decrease in the number of motorneurons, as well as somal atrophy and loss of dendritic arborization. Additionally, a loss of synaptic input from descending cortical motor neurons has also been observed [74, 77, 78].

The cellular pathology observed in MNDs is similar to that seen after axotomy or spinal cord injury. This supports the hypothesis that BDNF and other trophic signals from target musculature serve to maintain the neuromuscular unit [54, 56]. Muscle-synthesized BDNF may act as a positive feedback signal, increasing or maintaining the size and strength of the synapses formed between the motorneurons and the neurons of the motor cortex, which initiated the original muscle contraction [58, 60, 69, 70]. This feedback system may be directly affected in MND patients due, in part, to progressive muscle atrophy. Atrophied muscles may not release BDNF as robustly as healthy muscles do. In addition, a common component of neuropathy in patients with MND or spinal cord injury is disrupted retrograde transport, which would lead to a decrease in retrograde transport of muscle-synthesized BDNF. Disrupting the muscle signal, due to muscle atrophy as seen in disease, axotomy, or spinal cord injury, leads to specific, measurable markers of pathology in the motorneuron.

Our laboratory sought to further characterize the muscle source of BDNF, and its role in the maintenance of the motor unit. To address this, we have generated a strain of transgenic mice that are missing BDNF *specifically* in muscle fibers. The motorneurons of these mice were assessed for specific cellular markers commonly observed after spinal cord injury or in MNDs.

CHAPTER TWO: GENERATION, MAINTENANCE, AND PROCESSING OF EXPERIMENTAL TISSUE SAMPLES

Introduction

To generate experimental transgenic mice missing either one or both of the BDNF alleles in skeletal muscle, we used tissue-specific Cre-Lox recombination technology. This strategy takes advantage of the Cre-recombinase enzyme present in the virus bacteriophage P1. The enzyme will recognize and excise genomic DNA that is present between two 34-basepair regions – called loxP sites [79]. For our studies, we maintained one line of transgenic mice in which the coding region of the BDNF gene was flanked by two loxP sites. A second line of mice carrying the Cre-recombinase gene driven by the human skeletal actin promoter was also maintained. A detailed description of the mating scheme follows in the next section.

Methods

Animal Husbandry, Breeding, and Genotyping

All mice were housed in a temperature- and light-controlled room (14-h light, 10-h dark cycle; 21-23 ºC), and were provided with Mazuri Rodent Chow and water in excess. Mice were maintained according to NRC Guidelines for the Care and Use of Laboratory Animals. The Institutional Animal Care and Use Committee (IACUC) of Northern Michigan University approved all protocols.

The two strains of transgenic mice used for these experiments ($X^{Cre+}X^{Cre-}$, $BDNF^{Lox-/-}$; and $X^{Cre-}Y$, $BDNF^{Lox+/+}$; see Table 1) were obtained from Jackson Laboratories (Bar Harbor, ME). One strain contained loxP sites flanking one or both alleles of BDNF ($X^{Cre-}Y$, $BDNF^{Lox+/+}$). The second strain possessed an X-linked Cre-recombinase gene under the control

of the human skeletal actin (HSA) promoter ($X^{Cre+}X^{Cre-}$, $BDNF^{Lox-/-}$). Mice from each strain were bred to produce experimental animals lacking one or both copies of muscle-BDNF, as described below.

Initial F1 offspring were generated by crossing $X^{Cre+}X^{Cre-}$, $BDNF^{Lox-/-}$ females with $X^{Cre-}Y$, $BDNF^{Lox+/+}$ (Table 1). Male progeny ($X^{Cre+}Y$, $BDNF^{Lox+/-}$) were used as muscle$^{BDNF+/-}$ heterozygous knockouts. Female progeny ($X^{Cre+}X^{Cre-}$, $BDNF^{Lox+/-}$) were used for the experimental backcross described in the following paragraph.

$X^{Cre+}X^{Cre-}$, $BDNF^{Lox-/-}$ x $X^{Cre-}Y$, $BDNF^{Lox+/+}$				
	X^{Cre+}, $BDNF^{Lox-}$	X^{Cre+}, $BDNF^{Lox-}$	X^{Cre-}, $BDNF^{Lox-}$	X^{Cre-}, $BDNF^{Lox-}$
X^{Cre-}, $BDNF^{Lox+}$	$X^{Cre+}X^{Cre-}$, $BDNF^{Lox+/-}$	$X^{Cre+}X^{Cre-}$, $BDNF^{Lox+/-}$	$X^{Cre-}X^{Cre-}$, $BDNF^{Lox+/-}$	$X^{Cre-}X^{Cre-}$, $BDNF^{Lox+/-}$
X^{Cre-}, $BDNF^{Lox+}$	$X^{Cre+}X^{Cre-}$, $BDNF^{Lox+/-}$	$X^{Cre+}X^{Cre-}$, $BDNF^{Lox+/-}$	$X^{Cre-}X^{Cre-}$, $BDNF^{Lox+/-}$	$X^{Cre-}X^{Cre-}$, $BDNF^{Lox+/-}$
Y, $BDNF^{Lox+}$	$X^{Cre+}Y$, $BDNF^{Lox+/-}$	$X^{Cre+}Y$, $BDNF^{Lox+/-}$	$X^{Cre-}Y$, $BDNF^{Lox+/-}$	$X^{Cre-}Y$, $BDNF^{Lox+/-}$
Y, $BDNF^{Lox+}$	$X^{Cre+}Y$, $BDNF^{Lox+/-}$	$X^{Cre+}Y$, $BDNF^{Lox+/-}$	$X^{Cre-}Y$, $BDNF^{Lox+/-}$	$X^{Cre-}Y$, $BDNF^{Lox+/-}$

Table 1. Punnet square for experimental F1 cross. Female mice expressing Cre recombinase under the control of the human skeletal actin promoter ($X^{Cre+}X^{Cre-}$, $BDNF^{Lox-/-}$) were crossed with male mice expressing loxP sites surrounding both alleles of the BDNF gene ($X^{Cre-}Y$, $BDNF^{Lox+/+}$). The resulting male progeny ($X^{Cre+}Y$, $BDNF^{Lox+/-}$; highlighted in blue) were used as muscle$^{BDNF+/-}$ heterozygous knockouts. Female progeny ($X^{Cre+}X^{Cre-}$, $BDNF^{Lox+/-}$; highlighted in red) were used for the experimental backcross.

The experimental backcross was used to generate muscle$^{BDNF-/-}$ homozygous knockouts and muscle$^{BDNF+/+}$ controls. Female progeny from the F1 cross ($X^{Cre+}X^{Cre-}$, $BDNF^{Lox+/-}$) were bred with parental males ($X^{Cre-}Y$, $BDNF^{Lox+/+}$). The resulting male progeny ($X^{Cre+}Y$, $BDNF^{Lox+/+}$) were used as muscle$^{BDNF-/-}$ homozygous knockouts. Other male progeny ($X^{Cre-}Y$, $BDNF^{Lox+/+}$) were used as muscle$^{BDNF+/+}$ control mice (Table 2).

$X^{Cre+}X^{Cre-}$, $BDNF^{Lox+/-}$ x $X^{Cre-}Y$, $BDNF^{Lox+/+}$				
	X^{Cre+}, $BDNF^{Lox+}$	X^{Cre+}, $BDNF^{Lox-}$	X^{Cre-}, $BDNF^{Lox+}$	X^{Cre-}, $BDNF^{Lox-}$
X^{Cre-}, $BDNF^{Lox+}$	$X^{Cre+}X^{Cre-}$, $BDNF^{Lox+/+}$	$X^{Cre+}X^{Cre-}$, $BDNF^{Lox+/-}$	$X^{Cre-}X^{Cre-}$, $BDNF^{Lox+/+}$	$X^{Cre-}X^{Cre-}$, $BDNF^{Lox+/-}$
X^{Cre-}, $BDNF^{Lox+}$	$X^{Cre+}X^{Cre-}$, $BDNF^{Lox+/+}$	$X^{Cre+}X^{Cre-}$, $BDNF^{Lox+/-}$	$X^{Cre-}X^{Cre-}$, $BDNF^{Lox+/+}$	$X^{Cre-}X^{Cre-}$, $BDNF^{Lox+/-}$
Y, $BDNF^{Lox+}$	$X^{Cre+}Y$, $BDNF^{Lox+/+}$	$X^{Cre+}Y$, $BDNF^{Lox+/-}$	$X^{Cre-}Y$, $BDNF^{Lox+/+}$	$X^{Cre-}Y$, $BDNF^{Lox+/-}$
Y, $BDNF^{Lox+}$	$X^{Cre+}Y$, $BDNF^{Lox+/+}$	$X^{Cre+}Y$, $BDNF^{Lox+/-}$	$X^{Cre-}Y$, $BDNF^{Lox+/+}$	$X^{Cre-}Y$, $BDNF^{Lox+/-}$

Table 2. Punnet square for experimental backcross. Female mice expressing Cre recombinase under the control of the human skeletal actin promoter, and loxP sites surrounding one allele of the BDNF gene ($X^{Cre+}X^{Cre-}$, $BDNF^{Lox+/-}$) were crossed with male mice expressing loxP sites surrounding both alleles of the BDNF gene ($X^{Cre-}Y$, $BDNF^{Lox+/+}$). The resulting male progeny ($X^{Cre+}Y$, $BDNF^{Lox+/+}$; highlighted in green) were used as muscle$^{BDNF-/-}$ homozygous knockouts. Male progeny ($X^{Cre-}Y$, $BDNF^{Lox+/+}$; highlighted in orange) were used as muscle$^{BDNF+/+}$ control animals.

The resulting lines of transgenic mice are designated in this thesis as the following:

1) Muscle $^{BDNF\ +/+}$: Control mice (Genotype: $X^{Cre-}Y$, $BDNF^{Lox+/+}$) – Mice possess a functional BDNF gene in muscle tissue.
2) Muscle $^{BDNF\ +/-}$: Heterozygous knockouts (Genotype: $X^{Cre+}Y$, $BDNF^{Lox+/-}$) – Mice express one allele of BDNF in skeletal muscle.
3) Muscle $^{BDNF\ -/-}$: Homozygous knockouts (Genotype: $X^{Cre+}Y$, $BDNF^{Lox+/+}$) – Mice express no BDNF in skeletal muscle tissue.

Experimental and control animals were identified using PCR and gel electrophoresis. One set of primers used in PCR genotyping was used to verify the presence or absence of the loxP sites flanking the BDNF gene. The second set of primers determined the presence or absence of the Cre-recombinase gene (Figure 1).

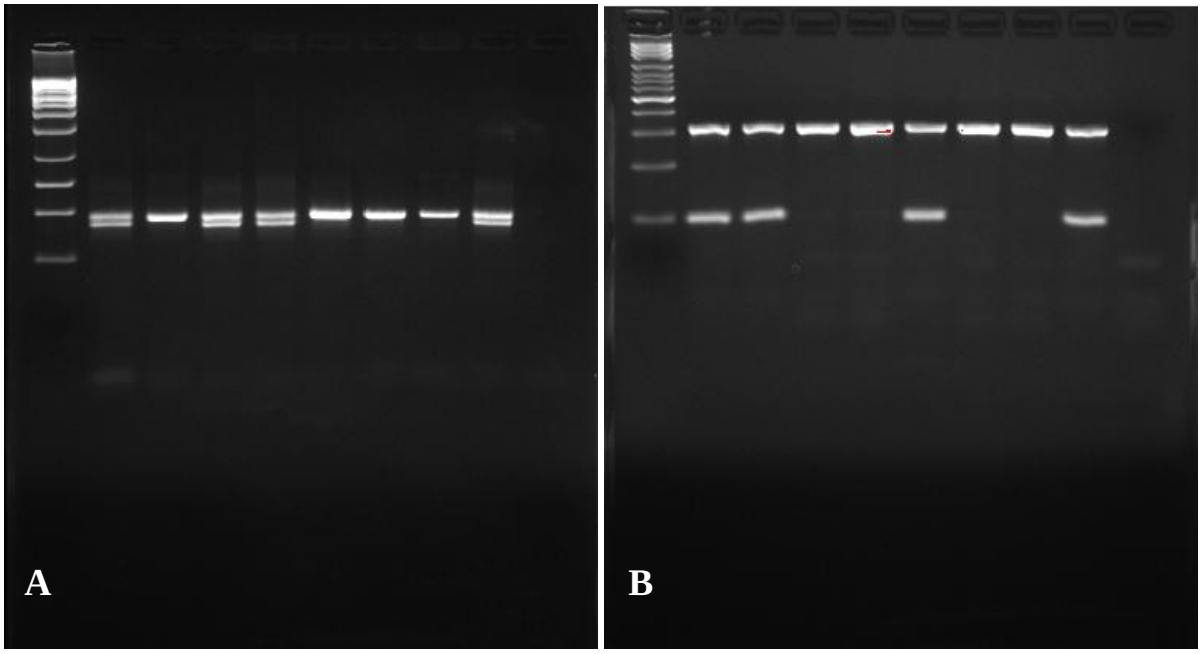

Figure 1. PCR Genotyping for Floxed BDNF and Cre-recombinase. (A) Primers were used to verify the presence or absence of loxP sites surrounding the BDNF coding exon. The PCR product of floxed alleles are 68 bp longer than the native PCR product. Animals that have one floxed allele and one native allele ($BDNF^{Lox+/-}$) display two bands after electrophoresis (lanes 2, 4, 5, and 9). Animals that have both alleles floxed ($BDNF^{Lox+/+}$) display one long band (lanes 3, 6, 7, and 8). (B) Primers were used to detect the presence or absence of the Cre-recombinase gene. Because this gene is non-native to mice, another set of primers were used to detect MOUSE GENE as a positive control. Animals expressing Cre recombinase ($X^{Cre+}Y$) display two bands (lanes 2, 3, 6, and 9). Animals negative for Cre-recombinase ($X^{Cre-}Y$) display only the positive control band (lanes 4, 5, 7, and 8).

To confirm that the Cre/Lox system in experimental transgenic mice knocked out the BDNF coding exon from muscles only, we performed PCR on tissue samples using primers that recognize genomic sequences upstream and downstream from the loxP sites flanking the BDNF coding exon. In the absence of HSA-Cre recombinase activity in $muscle^{BDNF+/+}$ controls, the PCR amplification product is approximately 2.45 kilobase-pairs (kbp) in length. If present in the muscles of experimental mice, Cre recombinase will remove a portion of the BDNF coding exon that is approximately 1.5 kbp in length. Thus, using the same primers, the PCR product amplified from skeletal muscles of $muscle^{BDNF-/-}$ animals is truncated to 950 bp in size. PCR analysis of skeletal muscles from $muscle^{BDNF+/-}$ experimental mice is expected to show both

banding patterns, as only one allele of the BDNF coding exon is floxed in these animals. The results of this PCR analysis of skeletal muscle and control tissue from experimental and control animals yielded expected results. In Figure 2, results demonstrate that an intact BDNF gene is present in quadriceps, kidney, heart, and brain tissue of muscle$^{BDNF+/+}$ control animals, as well as the kidney, heart, and brain tissue of muscle$^{BDNF-/-}$ homozygous knockout animals, indicated by the 2.45 kbp PCR product (lanes 2 through 5, and 7 through 9). In contrast, the quadriceps muscle of the same animal yielded a band approximately 950 bp in size (lane 6, asterisk). This banding pattern indicates that Cre recombinase was active only in skeletal muscle, and successfully knocked out the BDNF coding exon.

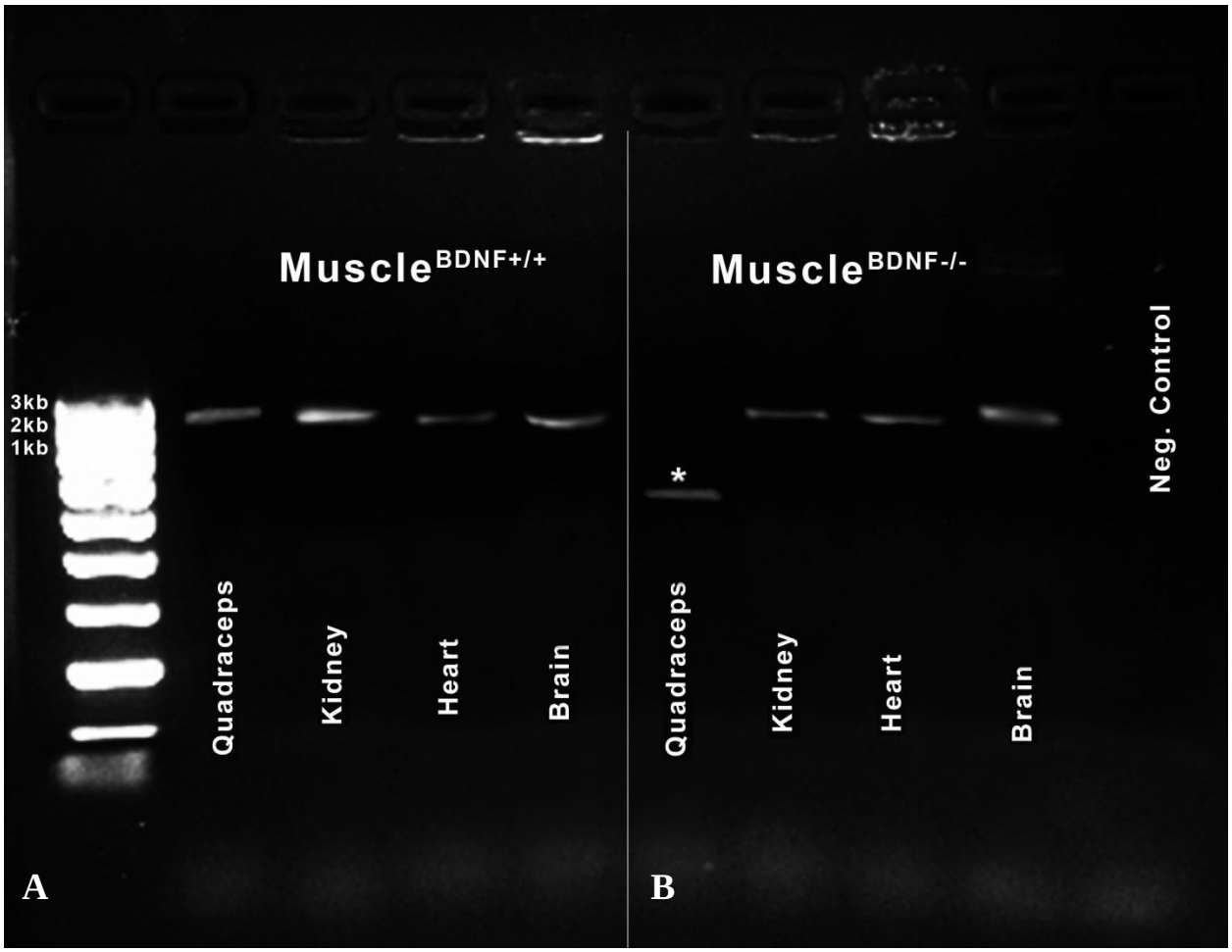

Figure 2. Cre recombinase activity is limited to the skeletal muscles of experimental mice. (A) Unaltered 2.45 kbp PCR product in quadriceps (lane 2), kidney (lane 3), heart (lane 4), and brain (lane 5) tissue of muscle$^{BDNF+/+}$ control mouse. (B) Truncated 950 bp PCR product in quadriceps (lane 6, asterisk), while unaltered 2.45 kbp band is detected in kidney (lane 7), heart (lane 8), and brain (lane 9) tissue of muscle$^{BDNF-/-}$ homozygous knockout animal.

Surgical Procedures and Tissue Processing

For histological and immunohistochemical studies, all mice from experimental and control genotypes at 30 d and 120 d time points underwent common procedures. Briefly, seven days prior to sacrifice, experimental and control animals received a 9 µL injection of Fluorogold (3% Fluorogold, 1% DMSO) into the gastrocnemius muscle under isofluorane anesthesia. The injection into the gastrocnemius consisted of three 3 µL injections into the distal, medial, and proximal regions of the muscle. Following injection, mice received a subcutaneous injection of

buprenorphine (0.3 mg/kg) for pain relief and were housed in clean single-mouse cages for recovery. Seven days after injection mice were euthanized by sodium pentabarbitol overdose – 0.4 µL injected intraperitoneally. Cardiac perfusion was performed with 4% paraformaldehyde. The spinal cords of perfused mice were harvested using pressured air and fixed overnight in 4% paraformaldehyde at 4 °C. Following fixation, spinal cords were stored in 30% sucrose in phosphate-buffered saline, pH 7.4 (PBS). The lumbar and cervical regions of the spinal cords were cut into 40 µm sections using a cryostat at -20 ºC. Lumbar sections were used in immunohistochemistry assays to determine if mice with missing or reduced muscle-synthesized BDNF exhibited differences in dendritic morphology and/or synaptic input. The cervical spinal cord sections were used to estimate motorneuron number and assess cell body morphology using standard histological assays.

CHAPTER THREE: A LACK OF MUSCLE-BDNF LEADS TO A DECREASE IN THE SOMAL AREA OF ASSOCIATED MOTORNEURONS.

Introduction

A marker of MNDs such as ALS is the progressive decrease in the number of motorneuron cell bodies by necrotic and apoptotic cell death. The remaining cell bodies begin to atrophy, which causes a decrease in soma size. Cell bodies can be visualized using thionin (Nissl stain), which specifically stains ribosomal RNA. Atrophied motorneurons, likes those of subjects affected by MNDs, do not pick up the Nissl stain as readily as healthy motorneurons.

We hypothesized that mice with missing or reduced muscle-synthesized BDNF would exhibit similar changes in motorneuron number and cell body size. If skeletal muscle provides trophic support to the motor unit via retrograde BDNF signaling, then motorneurons of muscle$^{BDNF+/-}$ heterozygous knockouts and muscle$^{BDNF-/-}$ homozygous knockouts should be reduced in number, display decreased cell body size, and exhibit lighter Nissl stain. We expected to see more significant signs of pathology in 120 d experimental mice compared to 30 d experimental mice.

Methods

Tissue preparation

Male 30 d (Muscle$^{BDNF-/-}$ n=8; Muscle$^{BDNF+/-}$ n=8; Muscle$^{BDNF+/+}$ n=8) and 120 d (Muscle$^{BDNF-/-}$ n=8; Muscle$^{BDNF+/-}$ n=8; Muscle$^{BDNF+/+}$ n=9) experimental and control mice were euthanized by a 0.4 mL intraperitoneal injection of sodium pentabarbitol, as described previously. Mice were then perfused with 40 mL ice-cold 0.9% saline, followed by 40 mL ice-cold 4% paraformaldehyde. Cervical spinal cords were harvested from perfused mice and post-

fixed in 4% paraformaldehyde for 2 hours and then impregnated with 30% sucrose in PBS at 4 ºC. After three days, they were cryostat sectioned at 40 µm and mounted on gelatin-subbed slides. They were stored at -20 ºC before thionin staining.

Thionin stain

Slides containing cervical spinal cord sections were immersed in distilled water for 5 minutes, then transferred to 0.04% thionin in acetate buffer for 15 minutes. The slides were washed twice in distilled water for 3 minutes and then dehydrated in ascending alcohol solutions (70%, 70%, 95%, and 100%) for 3 minutes each. The slides were cleared in Citrisolv for three minutes and then coverslipped using Cytoseal.

Microscopic Analysis

For each animal, 20-30 images containing several thionin-stained motorneuron cell bodies were taken at 40X magnification with a bright light microscope (Figure 3). An average of 85 total motorneurons were sampled for each animal in each genetic and age group. Using Olympus CellSens software, the area of each motorneuron soma in each image was determined by circumscribing a polygon around its perimeter. The average motorneuron cell body area was calculated for each age and genetic group. Average soma area for each age and genetic group was compared by one-way ANOVA and Bonferroni post-test using GraphPad Prism software. Data from both age groups were compared using two-way ANOVA and t-tests to compare the same genotype at two different ages. In addition to somal area, staining intensity was visually assessed and differences among genetic groups were noted.

Results and Discussion

Reduced or absent muscle-synthesized BDNF leads to a significant decrease in cell body size in both early (30 d) and mature (120 d) age groups. Figure 4 provides representative photomicrographs from 120 d mice from each genetic group. Visually, motorneurons from Muscle$^{BDNF+/-}$ heterozygous knockouts and Muscle$^{BDNF-/-}$ homozygous knockouts appear smaller, more fusiform or crenated, and have a lighter stain when compared to Muscle$^{BDNF+/+}$ control animals. The fusiform and/or crenated appearance observed in these motorneurons is a common indicator of neuropathy. These differences in appearance were also noted in 30 d mice.

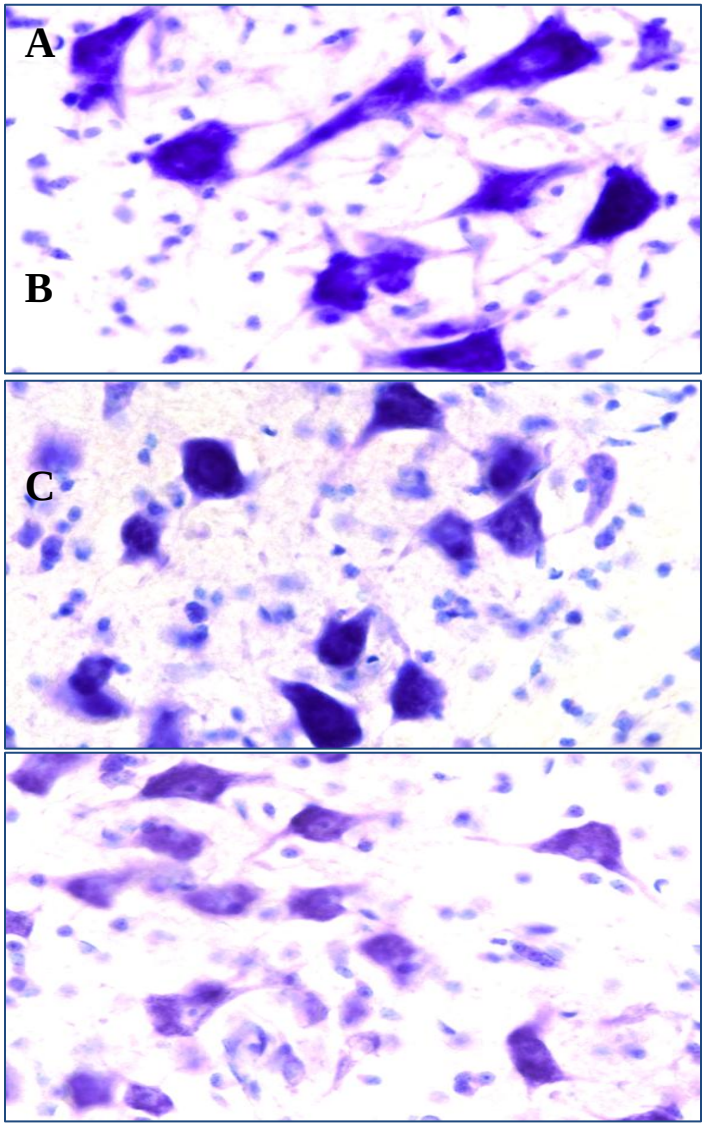

Figure 4. Somal atrophy in cervical spinal motorneurons. Representative 40X magnification photomicrograph of thionin Nissl-stained motor neurons in the cervical spinal cord from 120 d (A) Muscle$^{BDNF+/+}$ control mouse (B) Muscle$^{BDNF+/-}$ heterozygous knockout mouse and (C) Muscle$^{BDNF-/-}$ homozygous knockout mouse. Cell body area decreases across genetic groups. Notice that motorneurons from Muscle$^{BDNF+/-}$ and Muscle$^{BDNF-/-}$ animals (A and B) appear smaller, more fusiform, and stain much lighter when compared to Muscle$^{BDNF+/+}$ controls. This observation was made across all animals, at both 30 d and 120 d ages, although it was observed more intensely at 120 d. Additionally, note the likely vacuolation (indicated by the presence of white pockets) in the somata of Muscle$^{BDNF-/-}$ homozygous knockout animals.

Analysis revealed that at 30 d, Muscle$^{BDNF+/-}$ heterozygous knockout mice had significantly reduced soma size when compared to control of the same age ($p<0.01$; Figure 5A). Similarly, the motorneuron soma size of 30 d Muscle$^{BDNF-/-}$ homozygous knockout mice was significantly smaller compared to control ($p<0.001$; Figure 5B). At 120 d, both Muscle$^{BDNF+/-}$ heterozygous knockouts and Muscle$^{BDNF-/-}$ homozygous knockouts showed a similar decrease in cell body size when compared to Muscle$^{BDNF+/+}$ controls of the same age ($P<0.001$; Figure 5B).

Two-way ANOVA and t-tests revealed that both age and genetic group significantly affect soma size (Figure 6). In controls, soma size is significantly decreased at 120 d compared to 30 d ($P<0.05$). However, this decrease is more severe for Muscle$^{BDNF+/-}$ heterozygous knockouts ($P<0.01$), and there is no significant decrease from 30 d to 120 d in Muscle$^{BDNF-/-}$ homozygous knockouts.

As mentioned previously, it was noted that Muscle$^{BDNF+/-}$ heterozygous knockouts and Muscle$^{BDNF-/-}$ homozygous knockouts did display significantly lighter staining, as well as more cases of crenated or fusiform motorneuron cell bodies.

These results indicate that a muscle source of BDNF likely affects the somal morphology of innervating motorneurons. The dependence of somal morphology on a muscle-source BDNF may be less important at earlier ages. For example, while not significantly different from each other, the average somal area of motorneurons from 30 d Muscle$^{BDNF+/-}$ heterozygous knockouts is noticeably larger than that of Muscle$^{BDNF-/-}$ homozygous knockout mice (Figure 5A). By 120 d, the average soma size of motorneurons of both Muscle$^{BDNF+/-}$ and Muscle$^{BDNF-/-}$ have equalized (Figure 5B). At 30 d, the reduced amount of BDNF protein produced in the muscles in Muscle$^{BDNF+/-}$ mice may still provide adequate trophic support to motorneurons compared to the absence of muscle-synthesized BDNF by Muscle$^{BDNF-/-}$ mice. By 120 d, both heterozygous

knockout and homozygous knockouts display a similar decrease in size compared to controls, indicating that, with age, muscle-synthesized BDNF becomes more critical for trophic support of the motor unit. Indeed, previous behavior data (not shown) demonstrated that behavior deficits appear in these mice at 60-90d.

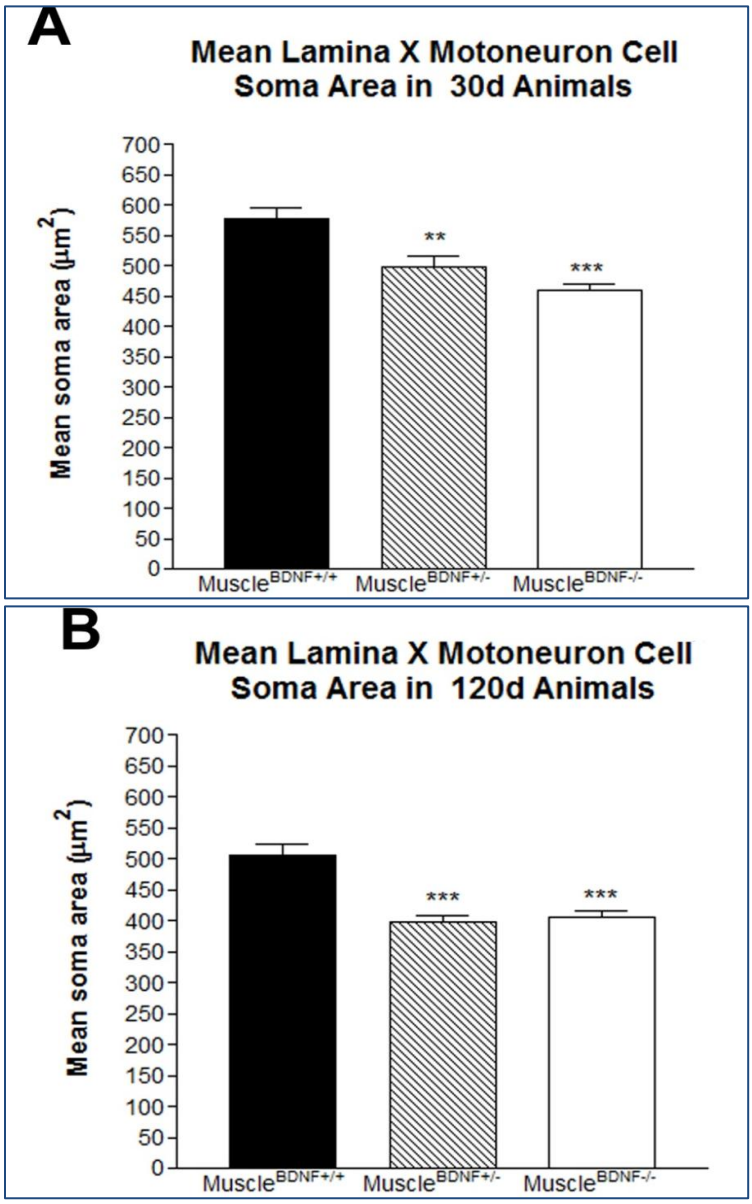

Figure 5. Somal atrophy in spinal motorneurons. One-way ANOVA comparing soma area of control mice to heterozygous knockout mice and homozygous knockout mice in (A) 30 d old and (B) 120 d old animals. (A) Mean soma area of 30 d Muscle$^{BDNF+/-}$ heterozygous knockout mice (**; $p<0.01$) and Muscle$^{BDNF-/-}$ homozygous knockout mice (***; $p<0.001$) is significantly decreased compared to Muscle$^{BDNF+/+}$ control animals. (B) Mean soma area of 120 d Muscle$^{BDNF+/-}$ heterozygous knockout mice (***; $p<0.001$) and Muscle$^{BDNF-/-}$ homozygous knockout mice (***; $p<0.001$) is significantly decreased compared to Muscle$^{BDNF+/+}$ control animals

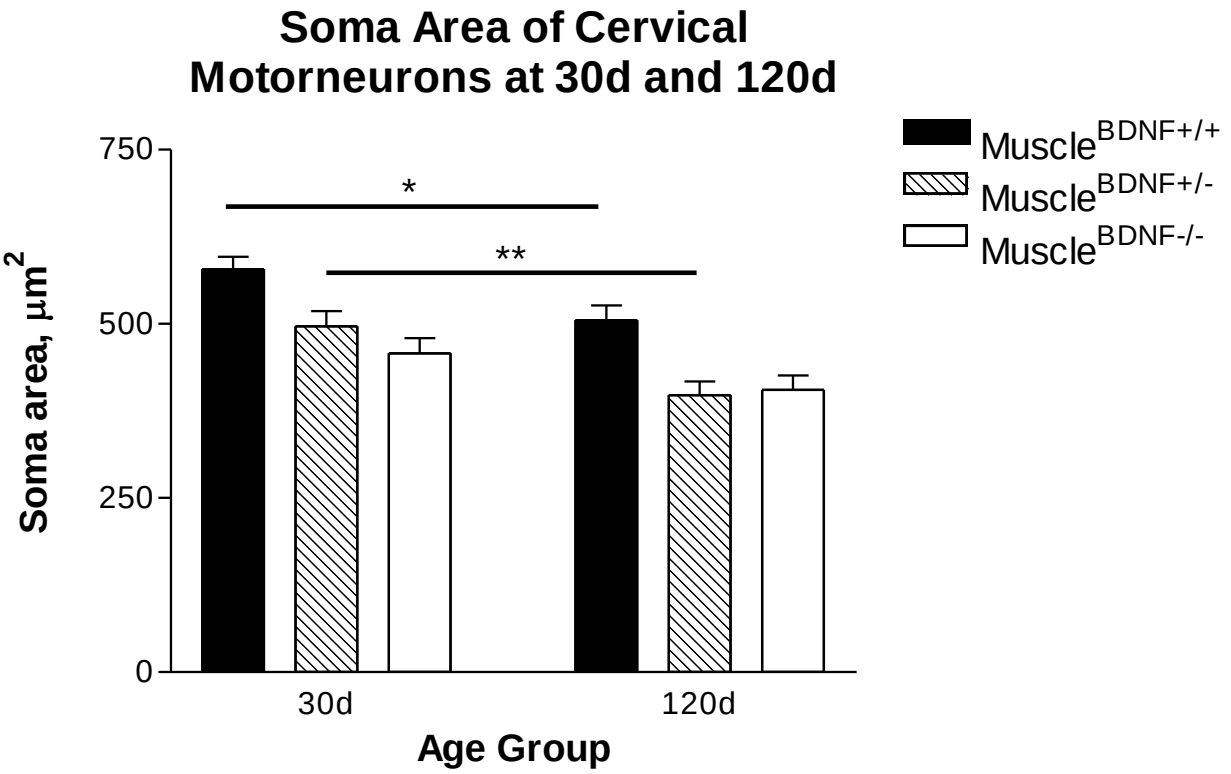

Figure 6. Two-way ANOVA comparing soma area at for all genetic groups at both 30 d and 120 d. Age and genetics both contribute to a progressive decrease in cell body size. Muscle$^{BDNF+/+}$ control animals exhibit reduced cell body area at 120 d compared to 30 d (*; $p<0.05$). Muscle$^{BDNF+/-}$ heterozygous knockout animals experience a more sever decrease in cell body size at 120 d compared to 30 d (**; $p<0.01$).

Conclusion

These data demonstrate that muscle-synthesized BDNF likely provides trophic support to maintain the size and health of motorneurons. This effect appears to be dose-dependent at an early life stage, as the somal size reduction is more drastic in Muscle$^{BDNF-/-}$ homozygous knockout mice than in Muscle$^{BDNF+/-}$ heterozygous knockout mice. At a later age, the reduction appears to be similar between these two groups. We observed crenated and fusiform cell bodies, in both knockout groups, resulting in a decrease in somal area. Future studies should address whether reduction in cell body size continues to progress at older ages. Analysis of motorneuron somata could include assessment for the presence of other pathological markers, including

ubiquitinated inclusions. Ubiquitin is used as a tag to mark vesicles containing proteins and other cellular material that is to be degraded. MND patients display a large number of these ubiquitinated inclusions in their motorneuron cell bodies. Additionally, cell body volume should be measured using the Imaris analysis software described below, as it would provide a measurement in three dimensions, rather than two. This would give us a more thorough description of size difference among cell bodies, and would provide a better image of their shape.

CHAPTER FOUR: BDNF PROTEIN EXPRESSION IS ALTERED IN MOTORNEURONS OF MICE WITH MISSING OR REDUCED MUSCLE-SYNTHESIZED BDNF.

Introduction

BDNF that is potentially transported retrogradely from skeletal muscle to motorneurons of the spinal cord may have a direct effect on the overall levels of the neurotrophin observed in the soma and dendrites. Additionally, retrograde BDNF signaling from skeletal muscle may influence transcription of the neurotrophin in motorneurons. Studies indicate that BDNF/TrkB binding can drive transcription of BDNF itself, along with other downstream targets [80]. We hypothesized that BDNF produced by muscles may influence levels of the neurotrophin in the motorneuron either by providing an exogenous source or by regulating transcriptional mechanisms, or both. If this hypothesis is true, reducing or eliminating skeletal muscle-BDNF should lead to a decrease in BDNF in the motorneuron cell body and dendrites. This system could be affected in patients with MNDs, due to poor signaling from atrophied muscles, decreased retrograde transport, or both. Using immunohistochemistry and laser-scanning confocal microscopy, the relative levels of BDNF protein in the motorneuron soma and dendrites of our experimental and control animals were assessed at two different ages. The antibodies used in the immunohistochemical assay labeled Fluorogold-labeled motorneuron cell bodies and dendrites and BDNF (used for colocalization analysis) as well as VGLUT1, which is a marker for synapses, and will be discussed in the next chapter.

Methods

Tissue preparation

One week before spinal cord harvest, under isofluorane anesthesia, the left gastrocnemius muscle of experimental animals was exposed by making an incision in the skin from Achilles tendon to the posterior knee joint. The gastrocnemius was then injected with 9 µL of the retrograde tracing molecule Fluorogold (3% Fluorogold, 1% DMSO, Fluorochrome, Inc., Denver, CO) – 3 µL each proximally, medially, and distally. Seven days after Fluorogold injection, mice were euthanized via 0.4 mL injection of sodium pentabarbitol intraperitoneally. After euthanasia, mice were perfused with 40 mL 0.9% saline, followed by 40 mL 4% paraformaldehyde. Lumbar spinal cords were harvested from 30 d and 120 d male mice after cardiac perfusion and post-fixed in 4% paraformaldehyde for 2 hours and then impregnated with 30% sucrose in phosphate-buffered saline at 4 ºC. After three days, they were cryostat sectioned at 40 µm and stored in cryoprotectant solution (10% sucrose in phosphate-buffered saline) for three days.

Immunohistochemistry

Lumbar spinal cord sections were washed with 1X phosphate-buffered saline, pH 7.4, three times for 10 minutes each and then incubated with blocking buffer (10% donkey serum, 0.2% triton, 0.1% sodium azide, in 1X PBS) at room temperature for one hour. Sections were then incubated with primary antibodies: 0.1% Rabbit polyclonal anti-Fluorogold; 0.2% Sheep polyclonal anti-BDNF; and 0.02% Guinea Pig polyclonal anti-VGLUT1 (EMD Millipore, Billerica, MA). Sections were incubated with primary antibodies on a rocking platform for 24 hours at room temperature then 24 hours at 4 ºC, after which they were washed again with 1X phosphate-buffered saline, pH 7.4, three times for 10 minutes each at room temperature.

Sections were incubated with secondary antibodies for one hour at room temperature: 1.3% AlexaFluor-488-conjugated Donkey anti-Rabbit IgG; 1.3% AlexaFluor-594-conjugated Donkey anti-Sheep IgG; and 1.3% AlexaFluor-647-conjugated Donkey anti-Guinea Pig IgG (Jackson ImmunoResearch, West Grove, PA). After secondary antibody incubation, sections were washed again with 1X phosphate-buffered saline, pH 7.4, three times for ten minutes each. The spinal cord sections were then mounted on to clean slides using a paintbrush. The slides were coverslipped using ProLong Gold Antifade Reagent (Invitrogen, Grand Island, NY), and stored in a light-proof box at 4 ºC.

Microscopic Analysis

Analysis was performed using an Olympus Fluoview confocal microscope (Olympus America, Center Valley, PA). For each scan, the image size was set to 800 x 800 pixels. Confocal images were obtained using either x40 or x60 oil immersion objective. Fluorogold-labeled motorneuron somata and dendrites were localized using epifluorescent (mercury vapor) illumination. Then we performed laser-scanning optical sectioning of the selected motorneurons. For each motorneuron (n = 20 per animal), we obtained 40-60 stacks of optical sections (Z step size = 0.54 µm for x40 objective; 0.45 µm for x60 objective). Each Z-series was composed of scans through three separate channels (488, 594, and 647 nm excitation). Scans at each wavelength were performed sequentially, to eliminate bleed-through between individual channels. All slices from each Z-series were compiled and these images were saved.

The images were imported to Imaris 7.6 program. The volume of any Fluorogold-labeled cell bodies within the image was defined using the Surfaces object. The automatic Surfaces Creation Wizard was used for this step. A region of interest containing the imaged cell bodies was selected, to avoid detection of background fluorescence. The source channel was set to

Channel 1 – AlexaFluor 488, the fluorophore used to label Fluorogold. Surface area detail level was set to 1 µm, which served to smooth out any roughness on the surface that was less than 1 µm in diameter. After running the Wizard, background fluorescence and poorly-labeled cell bodies were filtered out by filtering for a thresholded number of voxels value. This filter eliminated any surfaces that contained less voxels than the threshold value. If two or more cell bodies were close enough that their surfaces overlapped, these surfaces were cut using the Surfaces Toolkit, so that the cell body surface for each neuron was distinct.

The mean intensity of Channel 2 – AlexaFluor 594, the fluorophore used to label BDNF protein – colocalized to these surfaces was measured. These data were used as a means of comparing the amount of BDNF protein in motorneuron cell bodies between age and genetic groups. These data were compared by one-way ANOVA and Bonferroni post-test using GraphPad Prism software. Data from genetic groups at both 30 d and 120 d were analyzed using two-way ANOVA and t-tests.

Results and Discussion

At 30 d, there is no significant difference in the mean immunofluorescent intensity of BDNF in motorneuron cell bodies and dendrites of $Muscle^{BDNF+/+}$ control animals and $Muscle^{BDNF+/-}$ heterozygous knockout mice (Figure 7). These findings suggest that motorneurons of $Muscle^{BDNF+/-}$ experimental mice maintain normal expression of BDNF protein. In contrast, and somewhat surprisingly, BDNF immunofluorescent intensity is significantly increased in $Muscle^{BDNF-/-}$ homozygous knockout mice compared with $Muscle^{BDNF+/+}$ controls and $Muscle^{BDNF+/-}$ heterozygous knockouts ($P<0.001$; Figure 7).

Production of BDNF protein appears to be drastically increased in 30 d Muscle$^{BDNF-/-}$ motorneurons as a result of a total absence of the protein synthesized in muscles at this age. The most parsimonious explanation for this increase is a compensatory mechanism – i.e. motorneuron synthesis of BDNF is upregulated due to a lack of BDNF signaling from muscles.

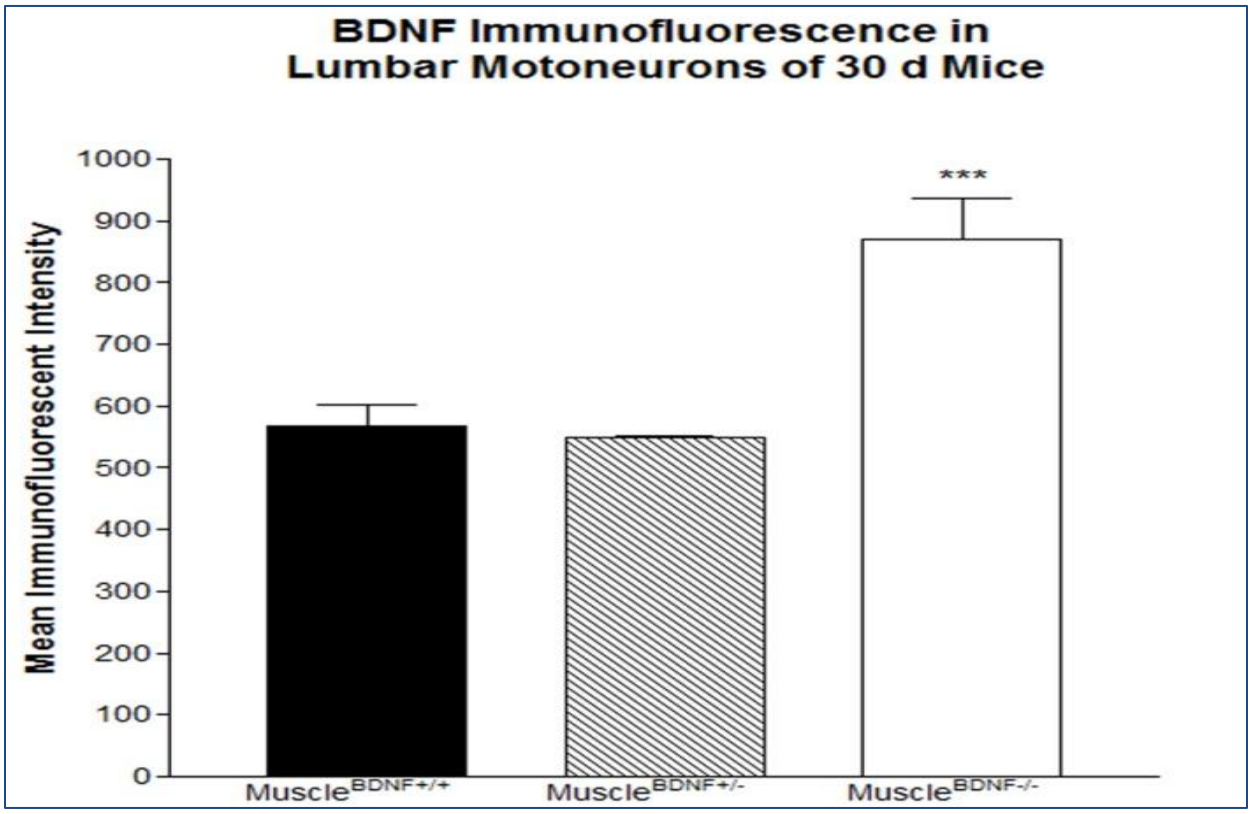

Figure 7. Expression of BDNF in motorneurons of 30 d mice. One-way ANOVA comparing mean BDNF immunofluorescent intensity in Fluorogold-labeled motorneurons Muscle$^{BDNF+/+}$, Muscle$^{BDNF+/-}$, and Muscle$^{BDNF-/-}$ mice. BDNF is significantly increased in Muscle$^{BDNF-/-}$ mice (***, $P<0.001$).

In mice at 120 d, expression patterns of BDNF in motorneurons are altered from the younger age. In contrast to 30 d mice, BDNF immunofluorescent intensity in motorneurons of 120 d Muscle$^{BDNF+/+}$ controls is not different than that of Muscle$^{BDNF-/-}$ homozygous knockout mice. However, BDNF immunofluorescent intensity in motorneurons from Muscle$^{BDNF+/-}$

heterozygous knockout mice is significantly higher than Muscle$^{BDNF-/-}$ homozygous mice and Muscle$^{BDNF+/+}$ control animals ($p<0.001$; Figure 8).

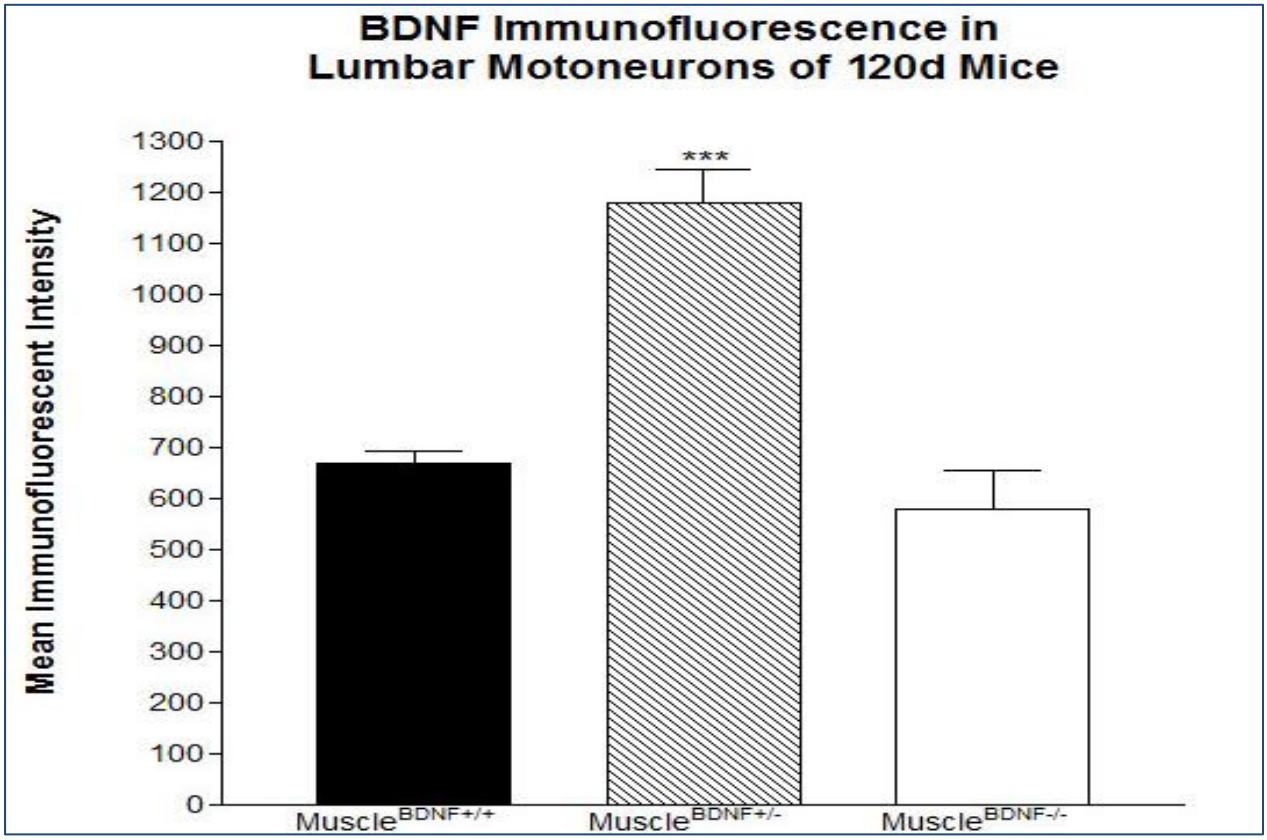

Figure 8. Expression of BDNF in motorneurons of 120 d mice. One way ANOVA comparing BDNF immunofluorescent mean intensity in Fluorogold-labeled motorneurons Muscle$^{BDNF+/+}$, Muscle$^{BDNF+/-}$, and Muscle$^{BDNF-/-}$ mice. BDNF is significantly increased in Muscle$^{BDNF+/-}$ mice (***, $P<0.001$).

Two-way ANOVA and t-tests revealed differences among all genetic groups when comparing 30 d to 120 d. BDNF immunofluorescent intensity was significantly higher in Muscle$^{BDNF+/+}$ control animals at 120 d compared to 30 d (Figure 9; $p<0.05$). This suggests that BDNF levels in motorneurons naturally increase with age. The results for Muscle$^{BDNF+/-}$ heterozygous animals and Muscle$^{BDNF-/-}$ homozygous animals did not trend this way, but BDNF levels were significantly different between age groups for both genetic groups (Figure 9; $p<0.0001$).

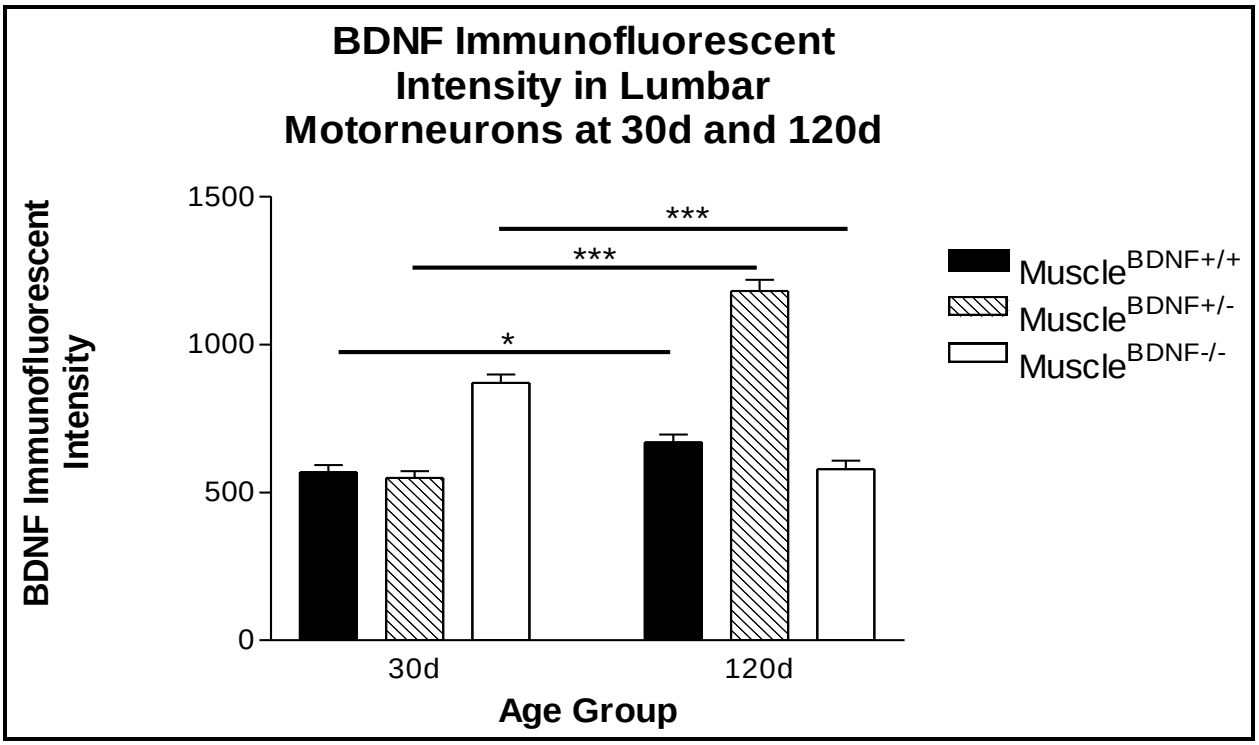

Figure 9. Two-way ANOVA of BDNF immunofluorescent intensity for all genetic groups at 30 d and 120 d. Muscle$^{BDNF+/+}$ control animals exhibit an increase in BDNF levels at 120 d compared to 30 d ($P<0.05$). Muscle$^{BDNF+/-}$ heterozygous knockout animals exhibit an increase in BDNF levels at 120 d compared to 30 d ($P<0.0001$). Muscle$^{BDNF-/-}$ homozygous knockout animals exhibit a decrease in BDNF levels at 120 d compared to 30 d ($P<0.0001$).

The change in expression patterns can be visualized in the representative confocal micrographs in Figure 10. The top panel of Figure 10 (A-C) displays micrographs from 30 d animals. Notice the intense yellow fluorescence (signifying colocalization of green and red fluorophores) in motorneurons of Muscle$^{BDNF-/-}$ animals (10C), in comparison to the green fluorescence in motorneurons of both Muscle$^{BDNF+/+}$ control animals (10A) and Muscle$^{BDNF+/-}$ heterozygous knockout animals (10B). The bottom panel of Figure 10 (D-F) displays representative micrographs from 120 d animals. At this age, we see intense yellow-labeled motorneurons from Muscle$^{BDNF+/-}$ heterozygous knockouts. In contrast, the motorneurons of both Muscle$^{BDNF-/-}$ homozygous knockouts and Muscle$^{BDNF+/+}$ controls appear green, indicative of a relatively low amount of overlap between green and red fluorophores.

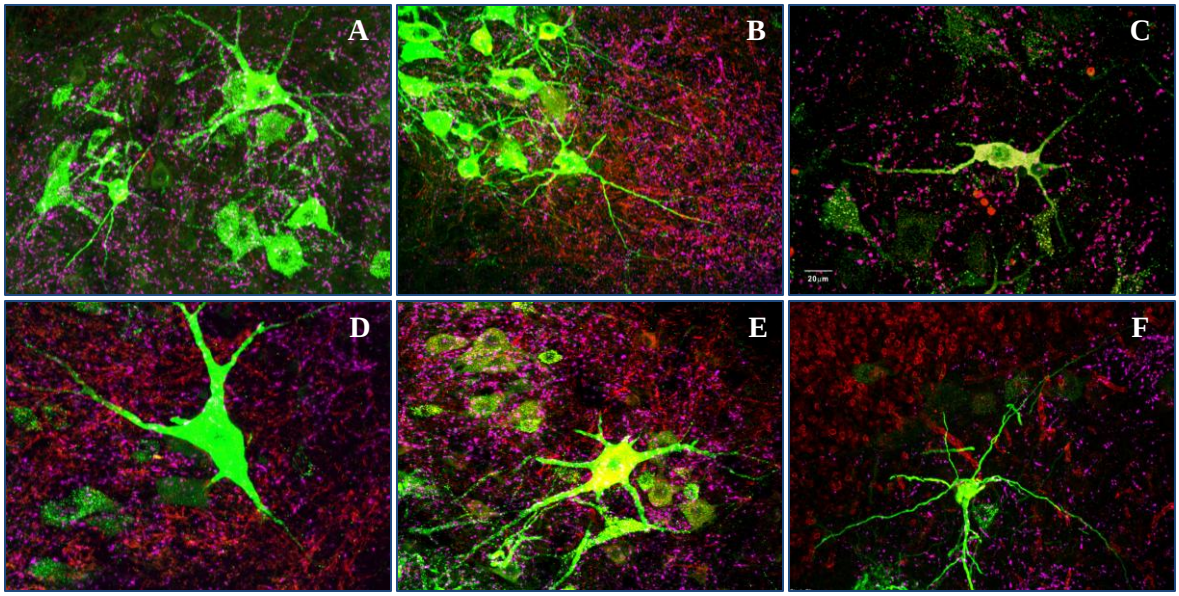

Figure 10. Neuropathological markers in motorneurons. Representative confocal micrograph of lumbar spinal cord sections immunoreactive for Fluorogold (green), BNDF (red) and VGLUT1 (magenta) in 30 d (A) Muscle$^{BDNF+/+}$, (B) Muscle$^{BDNF+/-}$, and (C) Muscle$^{BDNF-/-}$ mice; and in 120 d (D) Muscle$^{BDNF+/+}$, (E) Muscle$^{BDNF+/-}$, and (F) Muscle$^{BDNF-/-}$ mice. Note the intense yellow fluorescence in 8A and 8E – indicative of a high amount of overlap between red and green fluorophores. In 8C and 8F, we see additional examples of a small, crenated cell body, as described in Chapter 3.

These results suggest that at a young age (30 d), the reduction of muscle-synthesized BDNF in Muscle$^{BDNF+/-}$ mice does not influence BDNF levels in innervating motorneurons, which remain at levels of controls at this age. In contrast, motorneurons of 30 d Muscle$^{BDNF-/-}$ homozygous knockout mice exhibit a significant increase in BDNF immunofluorescent intensity compared to either Muscle$^{BDNF+/-}$ heterozygous knockout mice for Muscle$^{BDNF+/+}$ controls. At 30 d, the absence of BDNF produced by skeletal muscle in Muscle$^{BDNF-/-}$ mice seems to induce increased production of the neurotrophin by motorneurons, possibly as compensation for a reduced retrograde signal from muscles.

At a more mature age (120 d), the reduction of muscle-synthesized BDNF in Muscle$^{BDNF+/-}$ mice does appear to affect motorneuron synthesis of BDNF. These mice experience an increase of motorneuron-localized BDNF similar to that seen in 30 d Muscle$^{BDNF-/-}$

animals. Conversely, the motorneurons of Muscle$^{BDNF-/-}$ homozygous knockout animals display levels of BDNF protein near those of Muscle$^{BDNF+/+}$ control mice. At this later age, it appears that any compensatory increase in Muscle$^{BDNF-/-}$ homozygous knockout mice has waned, but that Muscle$^{BDNF+/-}$ heterozygous knockout are compensating.

Conclusion

From these data it can be concluded that muscle-synthesized BDNF affects expression of BDNF in motorneurons. A reduction or loss of BDNF from skeletal muscle appears to upregulate production of BDNF in motorneurons, although this happens at different ages depending on the amount of BDNF present in the muscles. It is possible that upregulation occurs in motorneurons once the consequences of muscle-synthesized BDNF loss reach a critical point. In homozygous knockouts, this occurs at an early age, due to the absence of BDNF. Normal BDNF levels appear to persist in motorneurons of heterozygous knockout mice for a longer period of time, due to the presence of some muscle-synthesized BDNF.

To further characterize this potential critical period, transgenic mice should be examined at several additional time points. Homozygous knockouts should be compared to controls and heterozygous knockouts at 10 d and 20 d to elucidate whether or not motorneuron levels of BDNF ever mimic those of controls, and if so, when the spike in BDNF production occurs. Heterozygous knockout mice should be compared to controls and homozygous knockouts between 30 d and 120 d (perhaps 60 d and 90 d) to again determine the point at which motorneuron levels of BDNF begin to rise. Determining BDNF expression by motorneurons at these ages will also allow us to understand whether the increase in BDNF production occurs gradually or spikes acutely. All mice should be examined beyond 120 d of age, to determine

whether BDNF levels eventually return to normal or if they are significantly reduced when compared to controls at a later age.

It can be hypothesized that in control animals, BDNF signaling from muscles to motorneurons helps to maintain a homeostatic level of BDNF expression. In the absence (at an early age) or reduction (at a mature age) of this signal, stress pathways are potentially activated that upregulate transcription and translation of BDNF. Because we see a drop in Muscle$^{BDNF-/-}$ homozygous knockouts at a later age, it can be assumed that after a period of compensatory upregulation, the activity of this pathway is reduced to levels comparable to control animals.

The mechanism behind this compensation is unclear. It is likely that trophic signals from intact motor units also feed back to cortical motorneurons. Because there is a loss of BDNF signal from muscle, the feedback to the motor cortex is disrupted. This may lead to increased stimulation of spinal motorneurons by cortical motorneurons. In cases of axotomy, spinal cord injury, or muscle atrophy, where there is a loss of connection between spinal motorneurons and their target musculature, an increase in excitatory cortical input is observed. It is possible that increased excitatory input from the cortical motorneurons leads to the compensatory increase in BDNF production by the motorneurons. The next step in addressing this issue would be two analyze the motorneurons for BDNF mRNA. This would elucidate whether the increased BDNF is being produced in the spinal motorneurons themselves, or imported from other areas, including cortical motorneurons or supporting glial cells. This could be done using in situ hybridization on spinal cord tissue or reverse-transcriptase polymerase chain reaction (RT-PCR).

CHAPTER FIVE: THE EFFECT OF ABSENT OR REDUCED MUSCLE-SYNTHESIZED BDNF ON DENDRITIC LENGTH, DIAMETER, AND SYNAPTIC INPUT.

Introduction

Progression of MNDs results in a loss of the dendritic arborization of the affected motorneurons. This in turn reduces the amount of excitatory synapses that these motorneurons receive from cortical areas and brain stem nuclei [81, 82]. We hypothesized that muscle-synthesized BDNF provides trophic support to innervating motorneurons, maintaining dendritic morphology and synapses. BDNF has been shown to maintain and promote growth of dendrites and synapses in several brain areas [6-9], thus, a similar function in the neuromuscular unit can be reasonably assumed. In mice with missing or reduced muscle-synthesized BDNF, a progressive decrease in dendritic length and diameter, and a reduction in synaptic input were predicted. We employed immunohistochemical techniques to visualize Fluorogold-labeled dendrites and VGLUT1 (a marker of excitatory synapses) to compare these morphological differences among age and genetic groups in our transgenic mice.

Methods

Tissue preparation

The tissue was prepared as described in Chapter Four. Under isofluorane anesthesia, the left gastrocnemius muscle of experimental animals was injected with 9 µL of the retrograde tracing molecule Fluorogold (3% Fluorogold, 1% DMSO, Fluorochrome, Inc., Denver, CO) – 3 µL each proximally, medially, and distally. Seven days after Fluorogold injection, lumbar spinal cords were harvested from 30 d and 120 d male mice after cardiac perfusion and post-fixed in 4% paraformaldehyde for 2 hours and then impregnated with 30% sucrose in phosphate-buffered

saline at 4 ºC. They were cryostat sectioned at 40 µm and stored in cryoprotectant solution (10% sucrose in phosphate-buffered saline) for three days.

Immunohistochemistry

The immunocytochemistry was done as described in Chapter Four. Lumbar spinal cord sections were washed with 1X phosphate-buffered saline, pH 7.4, three times for 10 minutes each and then incubated with blocking buffer (10% donkey serum, 0.2% triton, 0.1% sodium azide, in 1X PBS) at room temperature. Sections were then incubated with primary antibodies: 0.1% Rabbit polyclonal anti-Fluorogold; 0.2% Sheep polyclonal anti-BDNF; and 0.02% Guinea Pig polyclonal anti-VGLUT1 (EMD Millipore, Billerica, MA). Sections were incubated with primary antibodies for 24 hours at room temperature then 24 hours at 4 ºC, after which they were washed again with 1X phosphate-buffered saline, pH 7.4, three times for 10 minutes each at room temperature. Sections were incubated with secondary antibodies for one hour at room temperature: 1.3% AlexaFluor-488-conjugated Donkey anti-Rabbit IgG; 1.3% AlexaFluor-594-conjugated Donkey anti-Sheep IgG; and 1.3% AlexaFluor-647-conjugated Donkey anti-Guinea Pig IgG (Jackson ImmunoResearch, West Grove, PA). After secondary antibody incubation, sections were washed again with 1X phosphate-buffered saline, pH 7.4, three times for ten minutes each. They were then mounted on clean slides and coverslipped using ProLong Gold Antifade Reagent (Invitrogen, Grand Island, NY).

Confocal microscopy and image analysis

Analysis was performed using an Olympus Fluoview confocal microscope (Olympus America, Center Valley, PA). For each scan, the image size was set to 800 x 800 pixels. Confocal images were obtained using either x40 or x60 oil immersion objective. Fluorogold-labeled motorneuron somata and dendrites were localized using epifluorescent (mercury vapor)

illumination. Then we performed laser-scanning optical sectioning of the selected motorneurons. For each motorneuron (n = 20 per animal), we obtained 40-60 stacks of optical sections (Z step size = 0.54 µm for x40 objective; 0.45 µm for x60 objective). Each Z-series was composed of scans through three separate channels (488, 594, and 647 nm excitation). Scans at each wavelength were performed sequentially, to eliminate bleed-through between individual channels. All slices from each Z-series were compiled and these images were saved.

The images were imported to Imaris 7.6 program. The volume of Fluorogold-labeled cell bodies was defined the Surfaces function. Fluorogold-labeled dendrites were traced using Imaris Filament Tracer. Within the Filament Tracer menu, the semi-automatic "AutoPath" method was selected. This method requires the manual definition of seed points and terminal points of each dendritic branch. The cell bodies of neurons within the images were marked as seed points. Once end points were defined, the program automatically computed the path to the seed point. After all dendrites were traced, post-modification was done using the Filament Toolkit. The filament style was set to "cone", which automatically fills the diameter of the dendrite. The range was set to 1 µm to 18 µm (minimum and maximum diameter, respectively).

The Spots object was used to render synaptic terminals. The automatic Spots Creation Wizard was used for this step. The source channel was set to Channel 3 – AlexaFluor 647, which was the fluorophore used to label VGLUT1. The estimated XY diameter was set to 1.5 µm. After running the Wizard, the threshold was adjusted so that all synapses were detected, but no artificial synapses were detected. Using the MatLab program, we were able to detect and enumerate spots (synapses) making appositions on surfaces (cell bodies) and filaments (dendrites). This eliminated spots that were farther than 0.5 µm from surfaces or filaments. Several representative screen shots from this process can be seen in Figure 11.

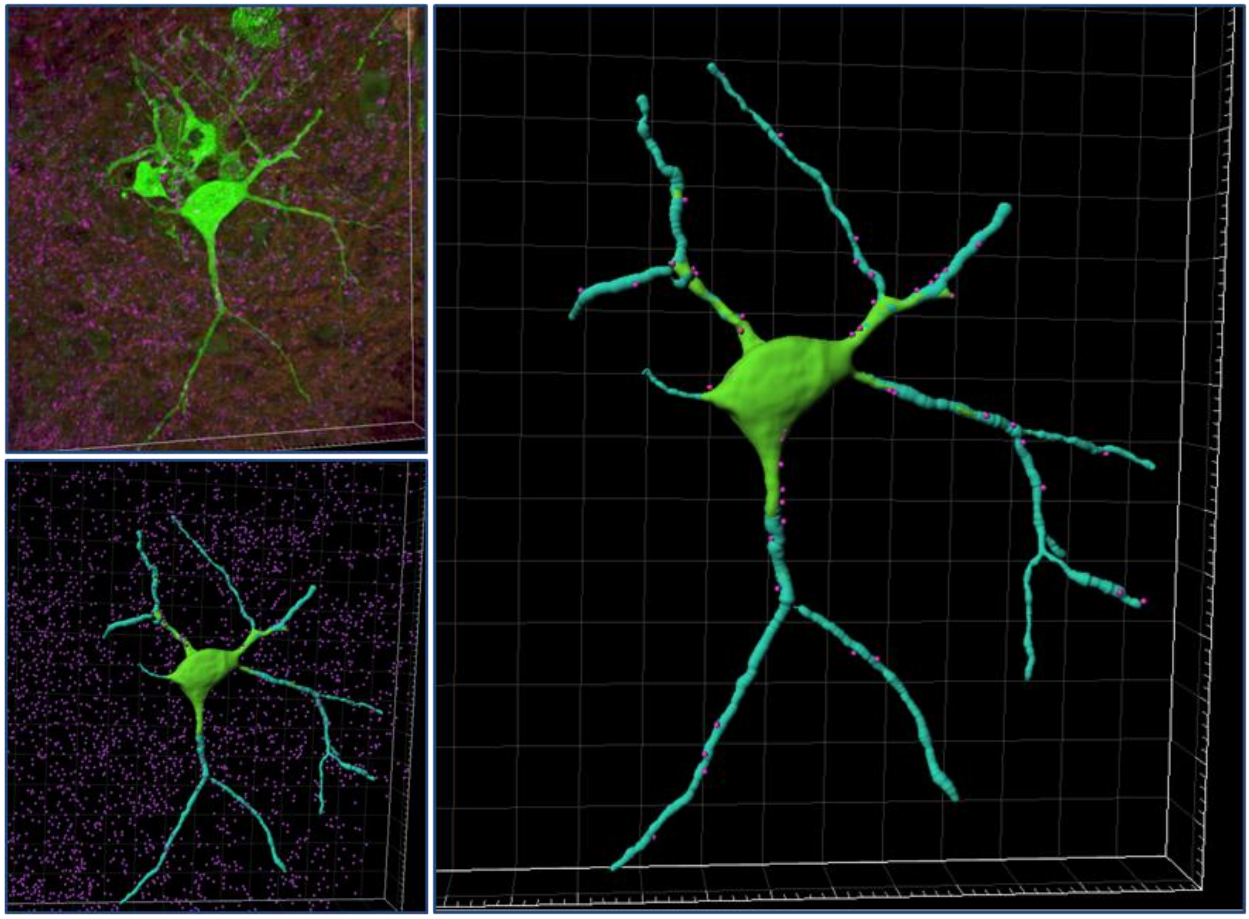

Figure 11. Imaris image analysis for dendritic length, diameter, and VGLUT1 synaptic input. (A) A confocal micrograph becomes a three dimensional rendering in which soma and dendrites are traced and filled to diameter, synapses are defined, and background structures are eliminated. (B) All synapses are eliminated except those making appositions on the motorneuron of interest.

For each image, data were collected on dendrite length, dendrite diameter, number of synapses apposing dendrites, and number of synapses apposing cell bodies. The data for dendrite length at 30 d were compared by one-way ANOVA and Bonferroni post-test GraphPad Prism. The data for dendrite length at 120 d were abnormally distributed. Thus, these data were compared within each age and genetic group by one-way ANOVA to ensure there was no significant difference between animals in each group. After this was completed, the lengths of all dendrites of all animals in a group were pooled, and the distribution of lengths was compared using a Kolmogorov-Smirnov (K-S) Test Comparison Plot. The groups compared using the K-S

test are listed in Table 3. The data for dendrite diameter apposed spots were each compared by one-way ANOVA and Bonferroni post-test using GraphPad Prism software.

Groups Compared in K-S Test	
30 d muscle$^{BDNF+/+}$ control	30 d muscle$^{BDNF+/-}$ heterozygous knockout
30 d muscle$^{BDNF+/+}$ control	30 d muscle$^{BDNF-/-}$ homozygous knockout
120 d muscle$^{BDNF+/+}$ control	120 d muscle$^{BDNF+/-}$ heterozygous knockout
120 d muscle$^{BDNF+/+}$ control	120 d muscle$^{BDNF-/-}$ homozygous knockout

Table 3. Groups compared in Kolmogorov-Smirnov (K-S) Comparison Plot. Four K-S tests were run. Each row describes the two groups compared with one another in a K-S test.

Results and Discussion

The data obtained for average dendritic length across all age and genetic groups were statistically compared using the Kolmogorov-Smirnov (K-S) test due to bimodal distribution of values in experimental groups, which could not be accurately analyzed by one-way ANOVA. The K-S test allowed us to pool the values for all animals in each genetic group and compare the distribution of values. The bimodal distribution was especially observed in the 120 d age group, which was analyzed first. The 30 d age group had a more normal distribution and was analyzed by one-way ANOVA.

At 30 d, there is a striking difference in the in the distribution of dendritic lengths of both Muscle$^{BDNF+/-}$ heterozygous knockouts and Muscle$^{BDNF-/-}$ homozygous knockouts, when compared with Muscle$^{BDNF+/+}$ control animals. One-way ANOVA reveals that Fluorogold-labeled dendrites of Muscle$^{BDNF+/-}$ heterozygous knockouts and Muscle$^{BDNF-/-}$ homozygous knockouts are significantly shorter compared to Muscle$^{BDNF+/+}$ control animals (Figure 12; $p<0.0001$). Additionally, Muscle$^{BDNF-/-}$ homozygous knockouts exhibit significantly shorter Fluorogold-labeled dendrites compared to Muscle$^{BDNF+/-}$ heterozyougs knockouts ($P<0.01$).

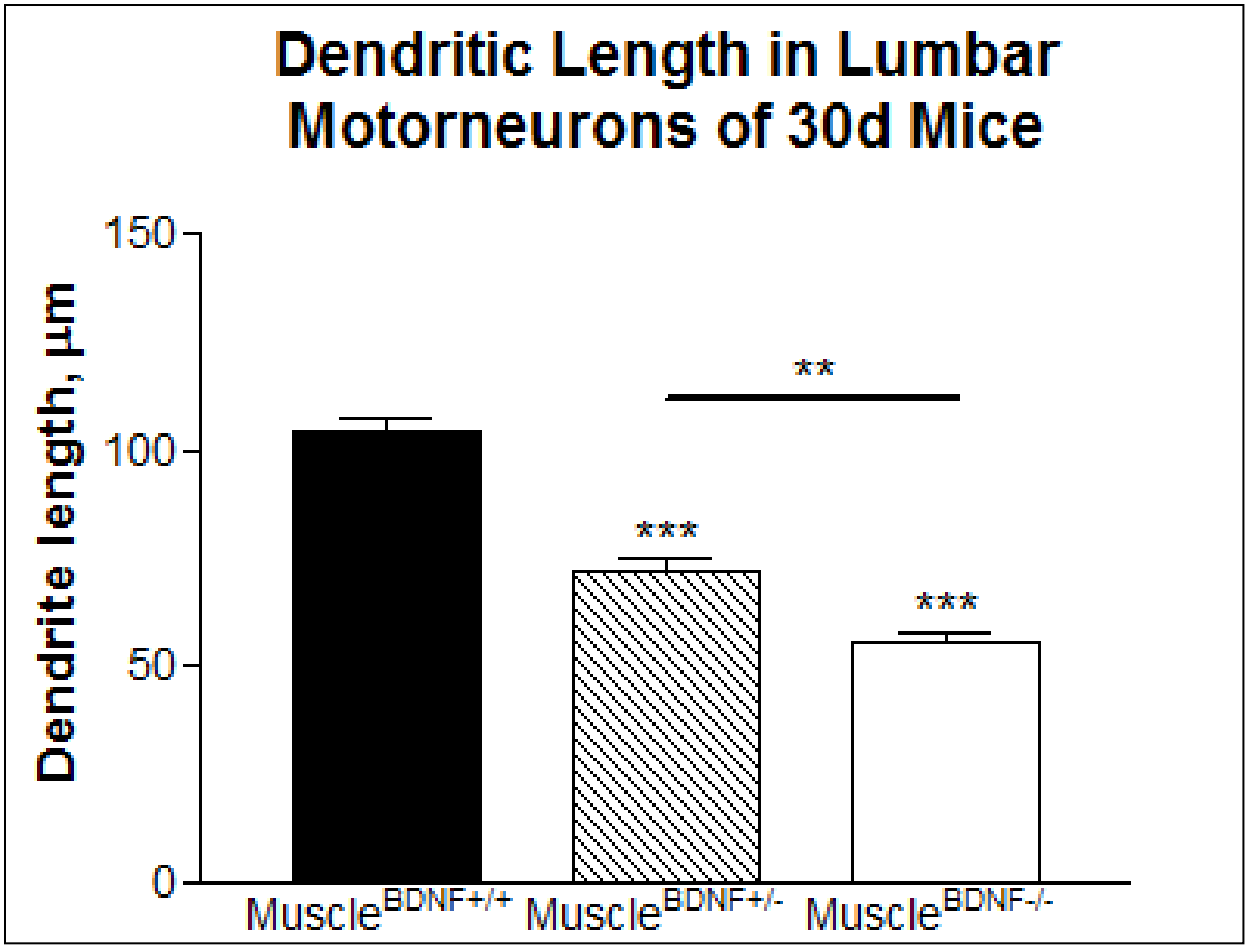

Figure 12. Decreased motorneuron dendritic length in 30 d mice with missing or reduced muscle-synthesized BDNF. One-way ANOVA comparing the distribution of dendritic length of 30 d Muscle$^{BDNF+/-}$ heterozygous knockouts to Muscle$^{BDNF+/+}$ control animals ($P<0.0001$); and Muscle$^{BDNF-/-}$ homozygous knockouts to Muscle$^{BDNF+/+}$ control animals ($P<0.0001$).

The K-S test allows us to view the differences between two samples at any given cumulative fraction (CF). At 120 d, the distribution of dendritic lengths is statistically different in both Muscle$^{BDNF+/-}$ heterozygous knockouts and Muscle$^{BDNF-/-}$ homozygous knockouts, when compared with Muscle$^{BDNF+/+}$ control animals. Control mice display a dendritic length around 50 µm in the 50th percentile (CF = 0.5). This number is 40 µm for both heterozygous knockouts and homozygous knockouts. The maximum dendritic length (CF = 1.0) for 120 d control animals is 235 µm for control animals. This is greatly reduced in experimental groups – 160 µm for heterozygous knockouts and 110 µm for homozygous knockouts. For 120 d heterozygous

knockouts compared with controls, D = 0.2432 (P<0.0001; Figure 13A). For 120 d homozygous knockouts compared with controls, D = 0.1582 (P<0.0001; Figure 13B).

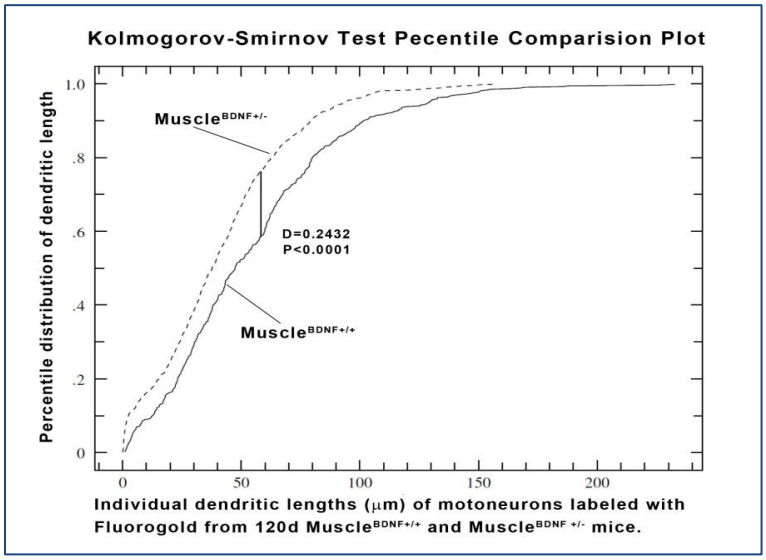

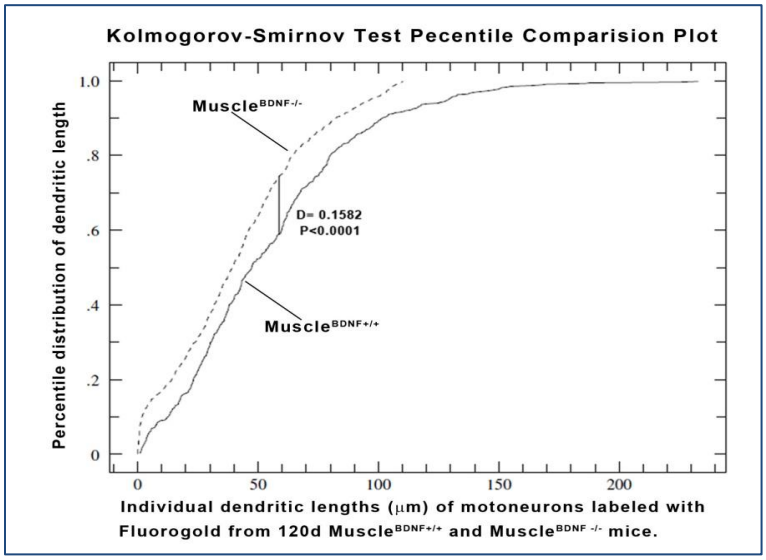

Figure 13. Differential motorneuron dendritic length in 120 d mice with missing or reduced muscle-synthesized BDNF. Kolmogorov-Smirnov Test comparing the distribution of dendritic length of 120 d (A) $Muscle^{BDNF+/-}$ heterozygous knockouts to $Muscle^{BDNF+/+}$ control animals (D=0.2432; P<0.0001); and (B) $Muscle^{BDNF-/-}$ homozygous knockouts to $Muscle^{BDNF+/+}$ control animals (D=0.1582; P<0.0001).

For each age group, we see a significant difference in dendritic length when comparing experimental mice to control mice. This difference is far more drastic in 30 d animals than in 120 d animals. This may seem counterintuitive, if the prediction of progressive pathology is made. However, if the role of BDNF in development is considered, then it stands to reason that reducing or eliminating one source of the protein would have a more severe effect at a younger

age. The neuromuscular unit of mice at 30 d of age could rely more heavily on trophic support of muscleBDNF than that of mice at 120 d of age, when development of the nervous system is complete. The comparison of dendrite length between control mice at 30 d and 120 d supports the idea that dendrites are still undergoing development at this stage. We see a linear distribution of dendrite lengths at 30 d, with a maximum length of 200 μm. At 120 d, we observe a more normal distribution of lengths, with a maximum length of 250 μm. Because of this difference, we can assume that the dendrites of 30 d mice are still undergoing development at this age.

These data specifically illustrate that there is a difference between the amount of Fluorogold labeling in motorneuron dendrites. The question arises whether this is due to a decrease in dendritic length, disrupted retrograde transport, or both. As mentioned previously, Fluorogold is a molecule that relies on the retrograde axonal transport system to fill, and therefore label, somata and dendrites of innervating motorneurons. Thus, the differences we observe initially suggest that dendrites are shorter in experimental animals, but they could also result from the inability of the motorneuron to transport Fluorogold retrogradely. This distinction needs to be made clear in further studies. Immunohistochemistry could be performed on the spinal cords of muscle-BDNF knockout mice for microtubule-associated protein 2 (MAP2) – a protein that is involved in microtubule assembly and enriched in dendrites. This technique would not rely on retrograde transport, and would thus be a more definitive measure of dendritic length differences. This cannot be concluded without further research, but it is probable that the observed effects are due to a disruption in retrograde transport, based on the observed dendritic lengths. The average length of lumbar motorneuron dendrites of adult mice about 2000 μm [83]. Our data find the maximum value at 250 μm, even in adult control mice. Thus, the dendrites are not being completely filled by the Fluorogold in the control nor the

experimental animals. It can be assumed, then, that the transport of the Fluorogold retrogradely is less efficient in mice with missing or reduced muscleBDNF.

One-way ANOVA reveals that, at 30 d, the mean diameter of Fluorogold-labeled dendrites are significantly decreased in Muscle$^{BDNF-/-}$ homozygous knockouts compared to Muscle$^{BDNF+/+}$ controls ($P<0.01$; Figure 14). There is no significant difference in dendritic diameter comparing Muscle$^{BDNF+/+}$ control animals to Muscle$^{BDNF+/-}$ heterozygous knockout animals.

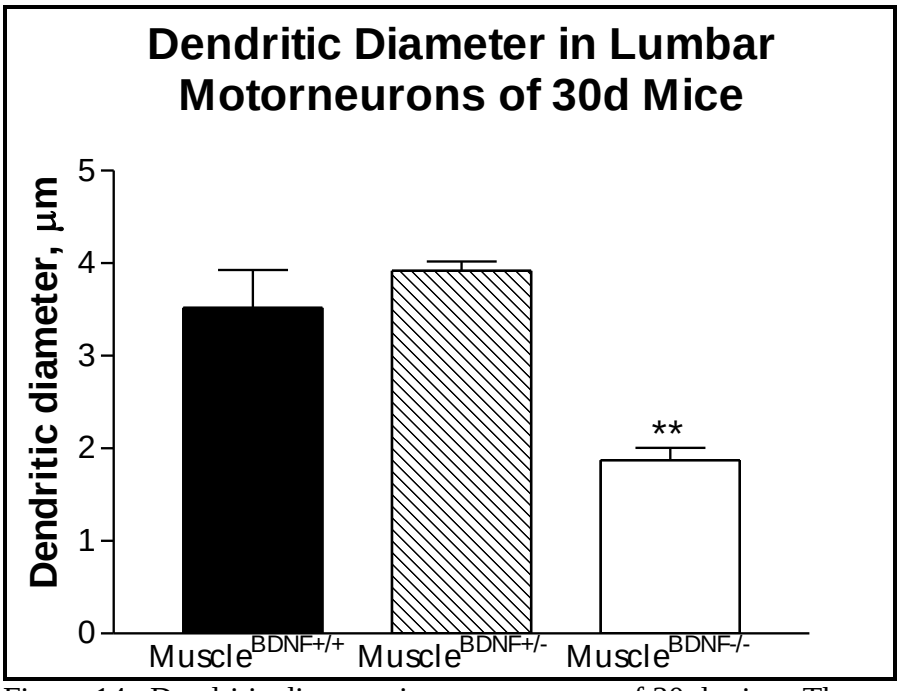

Figure 14. Dendritic diameter in motorneurons of 30 d mice. The mean diameter of Fluorogold-labeled dendrites is significantly decreased in Muscle$^{BDNF-/-}$ homozygous knockout animals compared to Muscle$^{BDNF+/+}$ controls and Muscle$^{BDNF+/-}$ heterozygous knockout mice (**; $P<0.01$).

One-way ANOVA reveals that, at 120 d, the mean diameter of Fluorogold-labeled dendrites are significantly decreased in both Muscle$^{BDNF+/-}$ heterozygous knockouts and Muscle$^{BDNF-/-}$ homozygous knockouts compared to Muscle$^{BDNF+/+}$ controls ($P<0.001$; Figure 15).

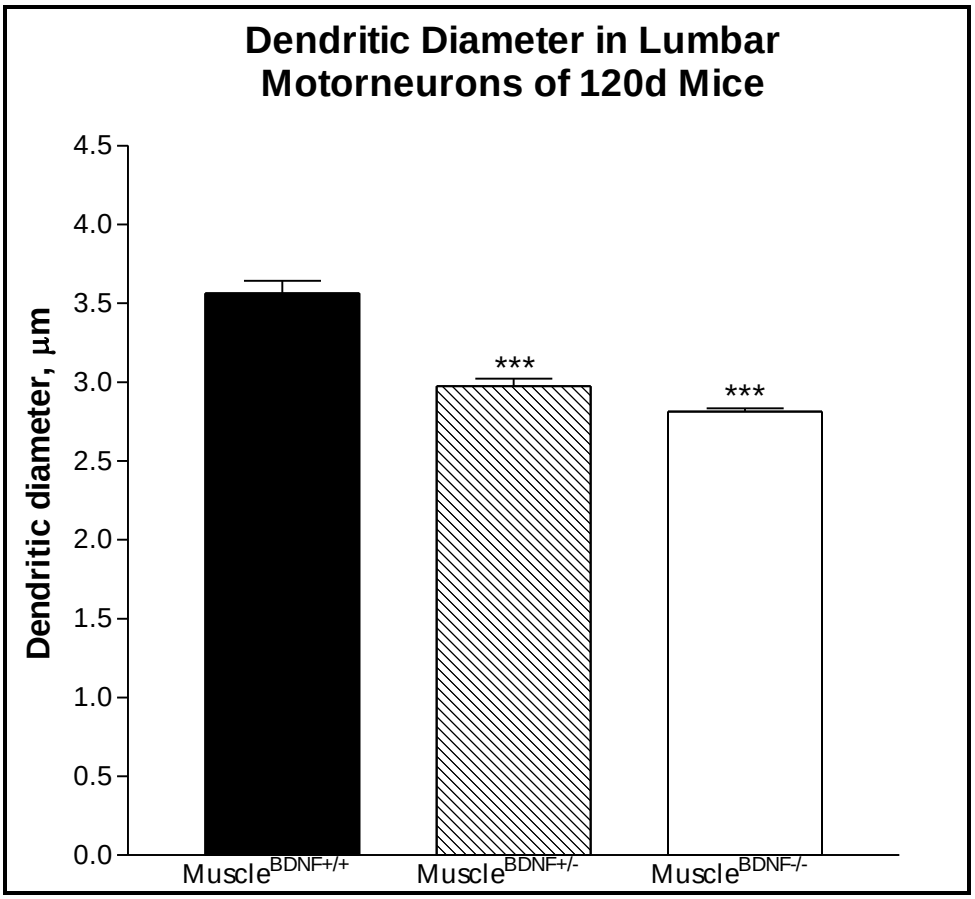

Figure 15. Reduced dendritic diameter in mice with missing or reduced muscle-synthesized BDNF. There is a significant decrease in both Muscle$^{BDNF+/-}$ heterozygous knockout animals and Muscle$^{BDNF-/-}$ homozygous knockout animals compared to Muscle$^{BDNF+/+}$ control animals (***; $P<0.001$).

The reduction we observe in dendritic diameter in both heterozygous knockout mice and homozygous knockout mice does not hold the same uncertainty as the dendritic length measurements. These differences cannot be attributed to disrupted retrograde transport, and thus are a strong indicator of atrophy of the dendritic arborization in mice with missing or reduced muscle-synthesized BDNF. In other neuronal networks, it has been well-characterized that target-derived BDNF activates the PI3K/Akt pathway to promote growth of dendrites and strengthen synapses. Our results suggest a similar mechanism in neuromuscular systems. It appears that without this target-derived source of BDNF, dendrites begin to atrophy.

The differences in the length of Fluorogold-labeled dendrites can be seen in Figure 16, which shows representative confocal micrographs from each age and genetic group.

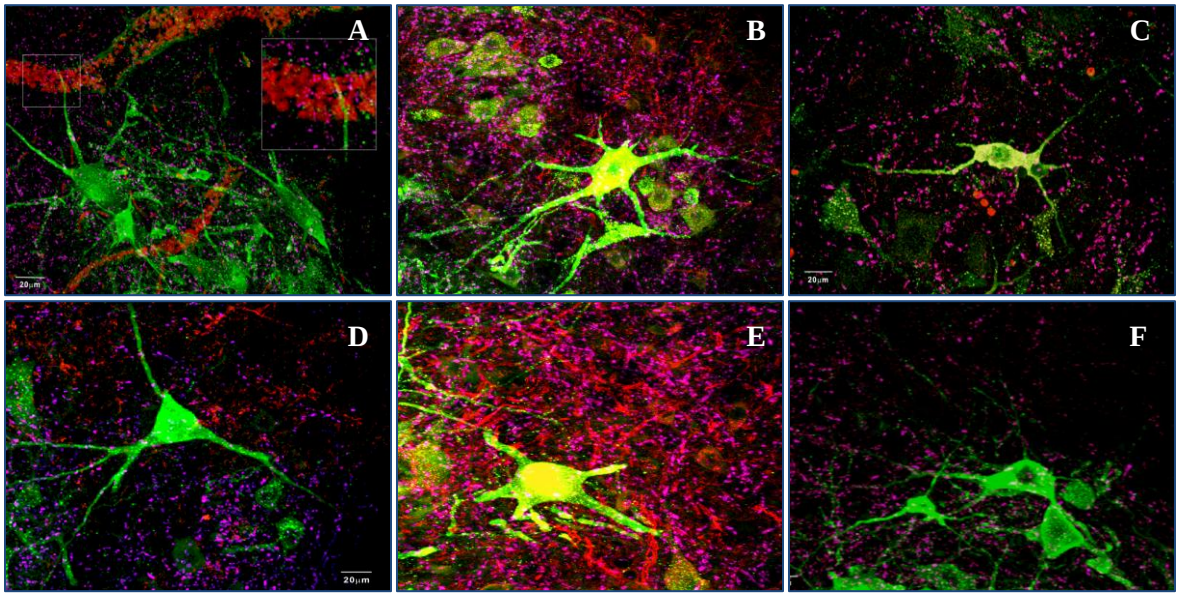

Figure 16. Neuropathological markers in motorneurons. Confocal micrograph of lumbar spinal cord sections immunoreactive for Fluorogold (green), BNDF (red) and VGLUT1 (magenta) in 30 d (A) Muscle$^{BDNF+/+}$ control animals, (B) Muscle$^{BDNF+/-}$ heterozygous knockouts, and (C) Muscle$^{BDNF-/-}$ homozygous knockouts; and 120 d (D) Muscle$^{BDNF+/+}$ control animals, (E) Muscle$^{BDNF+/-}$ heterozygous knockouts, and (F) Muscle$^{BDNF-/-}$ homozygous knockouts. Note the reduced length and diameter in knockout animals (B, C, E, F).

For each confocal micrograph, the dendritic synapses were enumerated, as well as the somal synapses. These numbers were highly variable. The total number of synapses for each neuron (dendritic appositions + somal appositions) was then compared by one-way ANOVA. There was no significant difference in the amount of VGLUT1-positive appositions among genetic groups at 120 d (Figure 17) or 30 d (not shown).

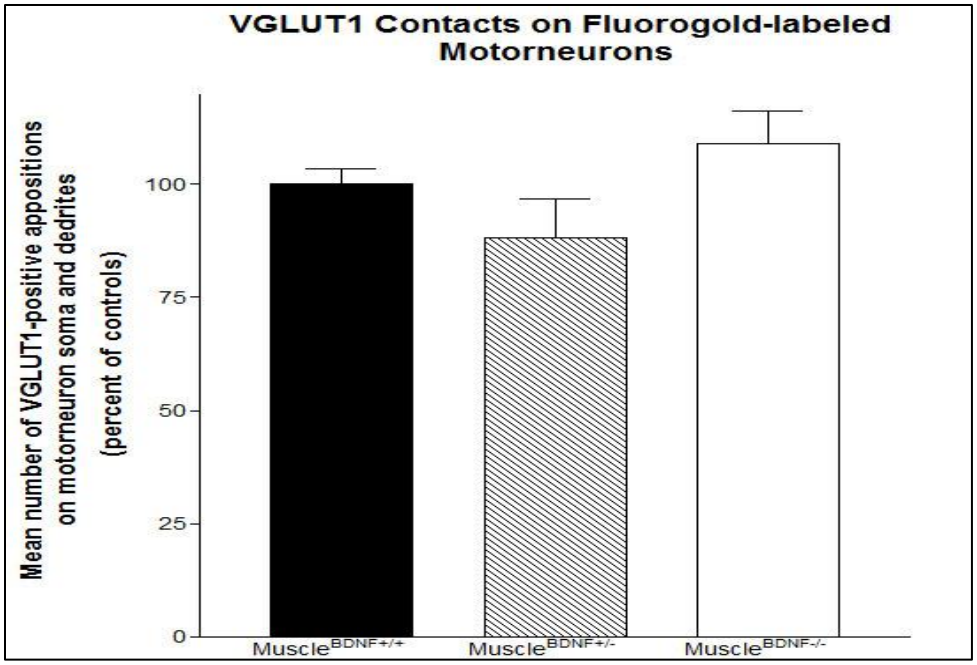

Figure 17. Mean number of VGLUT1 immunofluorescent appositions on Fluorogold labeled lumbar motoneurons. There was no significant difference in VGLUT1-positive contacts on motorneurons of 120 d Muscle$^{BDNF+/+}$ control, Muscle$^{BDNF+/-}$ heterozygous knockout, and Muscle$^{BDNF-/-}$ homozygous knockout mice.

The data collected via the Spots Object in Imaris 7.6 were highly variable. The values for number of synapses on a neuron ranged from 0 to 207. These results are not sufficient to conclude that there is actually not a difference in the synapses of mice with missing or reduced BDNF. The variability (and the fact that it is highly improbable that any neuron would have 0 synapses) suggests an error in the methodology. One parsimonious explanation is that the motorneurons, and more specifically their dendritic arbors, become caught, stretched, and/or displaced during cryostat sectioning. If this is the case, then simply labeling the postsynapse, rather than the presynapse, for postsynaptic density protein 95 (PSD-95) or NMDA receptors should produce more clear results.

Conclusion

From the present data, it may be concluded that muscle-synthesized BDNF acts retrogradely to provide trophic support to motorneurons and our data demonstrate that muscle-synthesized BDNF may help to maintain the retrograde axonal transport system. This could be achieved through the action of BDNF itself – for example, BDNF could act retrogradely to directly upregulate transcription of proteins involved in retrograde transport. Conversely, it may be indirectly affecting retrograde transport. Current studies in our laboratory report distinct pathology in the muscle fibers of Muscle$^{BDNF+/-}$ heterozygous knockout and Muscle$^{BDNF-/-}$ homozygous knockout mice. This pathology includes atrophy and hypertrophy of muscle fibers, fiber splitting, and centralized nuclei. Thus, healthy muscles might provide the motorneuron with some other diffusible factor that maintains the retrograde transport system – a factor that is not present or is ineffective in the degenerated muscle fibers of the muscle-BDNF knockouts. It is also possible that the retrograde transport system is not, in fact, disrupted. Instead, it could be that the dendrites actually are shorter in Muscle$^{BDNF+/-}$ heterozygous knockouts and Muscle$^{BDNF-/-}$ homozygous than in Muscle$^{BDNF+/+}$ controls. This explanation is less plausible than the former, as the largest dendrite measured in our analyses was about 250 μm in length, while the average motorneuron dendrite measures 2000 μm in length. The data collected for dendrite diameter do, in fact, indicate dendritic atrophy in both heterozygous knockout mice and homozygous knockout mice. As described in the Discussion section of this chapter, a different approach to labeling dendrites and synapses should be taken to get a better idea of differences in dendritic length and synaptic input.

CHAPTER SIX: SUMMARY, CONCLUSIONS, AND FUTURE DIRECTIONS

The present studies lay the groundwork for much more research concerning the role of muscle-synthesized BDNF in the health and maintenance of neuromuscular systems. Through our tissue-specific knockouts, we have presented evidence that muscle-synthesized BDNF provide trophic support retrogradely to innervating motorneurons.

In Chapter Three, we showed that muscle-synthesized BDNF directly affects the size of innervating cell bodies. We showed that eliminating or reducing muscle-BDNF leads to a decrease in cell body area, and that this effect is dose-dependent at an early life stage (30 d). The reduction appears not to be dose-dependent at a late life stage (120 d). Future studies should examine cell body size at more life stages – e.g. 10 d, 20 d, 60 d, 90 d, 150 d, and 210 d. It may also be useful to measure cell body volume using the Imaris Surfaces Object to analyze the three-dimensional confocal micrographs.

Chapter Four provides evidence that muscle-synthesized BDNF affects the production of itself in motorneuron cell bodies. This effect could be due to direct regulation by BDNF, or more likely due to other signals within the neuromuscular unit. Interestingly, we see an upregulation of motorneuron-synthesized BDNF as a result of reducing or eliminating muscle-synthesized BDNF at varying life stages depending upon whether muscle-synthesized BDNF is reduced or eliminated. This increase appears to be a compensatory response to stress, as it happens early for homozygous knockouts, and late for heterozygous knockouts. Thus, it is most likely not BDNF which directly regulates itself retrogradely in the motorneuron, but perhaps other signals that are released due to neuromuscular stress. With limited data, we conclude that there is a probable increase in BDNF production in the motorneuron at a critical time. The same

type of data needs to be collected from mice at more age groups (suggested above) to fully observe how muscle-BDNF affects the production of motorneuron-BDNF.

The objective of Chapter Five was to understand how muscle-synthesized BDNF affects the dendritic arborization and synaptic input of innervating motorneurons. Although we were unable to demonstrate this conclusively through our analysis of dendritic length and VGLUT1 labeling, it is likely that muscle-synthesized BDNF does, in fact, maintain dendrites and synapses. We did see changes in dendritic diameter in our knockout mice at both age groups, which cannot be attributed to disrupted retrograde transport. In light of these changes in diameter, and our conclusions about trophic support of the somata in Chapter Three and research performed to address BDNF's role in the synaptic signaling in the brain. Therefore, these objectives should be pursued as described in the Conclusion section of Chapter Five. For example, dendrites should be labeled with a dendrite specific antibody, such as MAP2. This method does not rely on retrograde transport, and so would allow us to definitively compare the length and diameter of dendrites across genetic and age groups. Synapses should be labeled with PSD-95, which would eliminate the possibility that dendrites are displaced away from their excitatory synapse during cryostat sectioning.

Chapter Five provides evidence that retrograde transport is disrupted in mice with missing or reduced muscle-BDNF. We observed a reduction in the length of Fluorogold-labeled dendrites in both heterozygous and homozygous muscle-BDNF knockouts. Because the tracing molecule Fluorogold relies on the retrograde transport system, and because our measured lengths are much shorter than the average lumbar spinal cord motorneuron dendritic length, we can reasonably assume that the differences may be due to disrupted transport. This transport system may be regulated by BDNF directly, or it may be that other transcription factors responsible for

the maintenance of this system are negatively affected by unhealthy muscle fibers and motorneurons.

We can conclude that the muscle source of BDNF is integral to the maintenance of the neuromuscular unit, although the exact mechanisms by which it does this remain unknown. A reduction or loss of this protein from skeletal muscle leads to several cellular markers also present in neuromuscular diseases. This trophic support system from muscles may be disrupted or affected in a multitude of human neuromuscular diseases in which muscle fibers are atrophied. Any retrograde trophic signal from muscle will be reduced when fibers are atrophied. Moreover, these results mimic results seen in models of spinal cord injury and axotomy, were the connection between motorneurons and target musculature is disrupted. This provides evidence that BDNF is one of the important diffusible factors that is affected in these models. In addition to the further experimentation described above, research should be proposed and performed to fully understand role of BDNF produced in the muscle. This includes a complete analysis of muscle fiber pathology at all life stages, an analysis of the neuromuscular junction, and characterization of behavioral pathology in muscle-BDNF knockout mice. If this pathology matches or mimics that of neuromuscular diseases, then exogenous BDNF applied at the neuromuscular junction could be considered as a viable treatment option for such diseases. Further, the mechanism by which muscle-synthesized BDNF supports and maintains the motor unit should be described. Future studies should examine the gene transcription pathways activated by muscle-synthesized BDNF/TrkB binding. Again, it is uncertain whether some of the effects we see are directly related to BDNF/TrkB signaling, or if they are the result of a loss of other signaling molecules due to atrophied muscle fibers and motorneurons. Thus, the downstream targets of muscle-synthesized BDNF in the motorneurons should be elucidated.

REFERENCES

1. Sakuma, K. and A. Yamaguchi, *The recent understanding of the neurotrophin's role in skeletal muscle adaptation.* J Biomed Biotechnol, 2011. **2011**: p. 201696.
2. Griesbeck, O., et al., *Expression of neurotrophins in skeletal muscle: quantitative comparison and significance for motoneuron survival and maintenance of function.* J Neurosci Res, 1995. **42**(1): p. 21-33.
3. Chevrel, G., R. Hohlfeld, and M. Sendtner, *The role of neurotrophins in muscle under physiological and pathological conditions.* Muscle Nerve, 2006. **33**(4): p. 462-76.
4. Hata, Y., T. Tsumoto, and M.P. Stryker, *Selective pruning of more active afferents when cat visual cortex is pharmacologically inhibited.* Neuron, 1999. **22**(2): p. 375-81.
5. Singh, K.K., et al., *Developmental axon pruning mediated by BDNF-p75NTR-dependent axon degeneration.* Nat Neurosci, 2008. **11**(6): p. 649-58.
6. Huang, Z., *Molecular regulation of neuronal migration during neocortical development.* Mol Cell Neurosci, 2009. **42**(1): p. 11-22.
7. Huang, E.J. and L.F. Reichardt, *Neurotrophins: roles in neuronal development and function.* Annu Rev Neurosci, 2001. **24**: p. 677-736.
8. Zhou, B., et al., *Snapin recruits dynein to BDNF-TrkB signaling endosomes for retrograde axonal transport and is essential for dendrite growth of cortical neurons.* Cell Rep, 2012. **2**(1): p. 42-51.
9. Lu, B., P.T. Pang, and N.H. Woo, *The yin and yang of neurotrophin action.* Nat Rev Neurosci, 2005. **6**(8): p. 603-14.
10. Kang, H. and E.M. Schuman, *A requirement for local protein synthesis in neurotrophin-induced hippocampal synaptic plasticity.* Science, 1996. **273**(5280): p. 1402-6.
11. Duman, R.S., *Pathophysiology of depression: the concept of synaptic plasticity.* Eur Psychiatry, 2002. **17 Suppl 3**: p. 306-10.
12. Stoop, R. and M.M. Poo, *Synaptic modulation by neurotrophic factors: differential and synergistic effects of brain-derived neurotrophic factor and ciliary neurotrophic factor.* J Neurosci, 1996. **16**(10): p. 3256-64.
13. Schinder, A.F. and M. Poo, *The neurotrophin hypothesis for synaptic plasticity.* Trends Neurosci, 2000. **23**(12): p. 639-45.
14. Ou, L.C. and P.W. Gean, *Regulation of amygdala-dependent learning by brain-derived neurotrophic factor is mediated by extracellular signal-regulated kinase and phosphatidylinositol-3-kinase.* Neuropsychopharmacology, 2006. **31**(2): p. 287-96.
15. Rattiner, L.M., et al., *Brain-derived neurotrophic factor and tyrosine kinase receptor B involvement in amygdala-dependent fear conditioning.* J Neurosci, 2004. **24**(20): p. 4796-806.
16. Rattiner, L.M., M. Davis, and K.J. Ressler, *Differential regulation of brain-derived neurotrophic factor transcripts during the consolidation of fear learning.* Learn Mem, 2004. **11**(6): p. 727-31.
17. Chhatwal, J.P., et al., *Amygdala BDNF signaling is required for consolidation but not encoding of extinction.* Nat Neurosci, 2006. **9**(7): p. 870-2.
18. Horch, H.W. and L.C. Katz, *BDNF release from single cells elicits local dendritic growth in nearby neurons.* Nat Neurosci, 2002. **5**(11): p. 1177-84.

19. Drake, C.T., T.A. Milner, and S.L. Patterson, *Ultrastructural localization of full-length trkB immunoreactivity in rat hippocampus suggests multiple roles in modulating activity-dependent synaptic plasticity.* J Neurosci, 1999. **19**(18): p. 8009-26.
20. Bramham, C.R. and E. Messaoudi, *BDNF function in adult synaptic plasticity: the synaptic consolidation hypothesis.* Prog Neurobiol, 2005. **76**(2): p. 99-125.
21. Tongiorgi, E., M. Righi, and A. Cattaneo, *Activity-dependent dendritic targeting of BDNF and TrkB mRNAs in hippocampal neurons.* J Neurosci, 1997. **17**(24): p. 9492-505.
22. Schuman, E.M., J.L. Dynes, and O. Steward, *Synaptic regulation of translation of dendritic mRNAs.* J Neurosci, 2006. **26**(27): p. 7143-6.
23. Righi, M., E. Tongiorgi, and A. Cattaneo, *Brain-derived neurotrophic factor (BDNF) induces dendritic targeting of BDNF and tyrosine kinase B mRNAs in hippocampal neurons through a phosphatidylinositol-3 kinase-dependent pathway.* J Neurosci, 2000. **20**(9): p. 3165-74.
24. Rex, C.S., et al., *Brain-derived neurotrophic factor promotes long-term potentiation-related cytoskeletal changes in adult hippocampus.* J Neurosci, 2007. **27**(11): p. 3017-29.
25. Noble, E.E., et al., *The lighter side of BDNF.* Am J Physiol Regul Integr Comp Physiol, 2011. **300**(5): p. R1053-69.
26. Conner, J.M., et al., *Distribution of brain-derived neurotrophic factor (BDNF) protein and mRNA in the normal adult rat CNS: evidence for anterograde axonal transport.* J Neurosci, 1997. **17**(7): p. 2295-313.
27. Lom, B. and S. Cohen-Cory, *Brain-derived neurotrophic factor differentially regulates retinal ganglion cell dendritic and axonal arborization in vivo.* J Neurosci, 1999. **19**(22): p. 9928-38.
28. Mirabella, N., et al., *Effects of castration on the expression of brain-derived neurotrophic factor (BDNF) in the vas deferens and male accessory genital glands of the rat.* Cell Tissue Res, 2006. **323**(3): p. 513-22.
29. Cosker, K.E., S.L. Courchesne, and R.A. Segal, *Action in the axon: generation and transport of signaling endosomes.* Curr Opin Neurobiol, 2008. **18**(3): p. 270-5.
30. Ginty, D.D. and R.A. Segal, *Retrograde neurotrophin signaling: Trk-ing along the axon.* Curr Opin Neurobiol, 2002. **12**(3): p. 268-74.
31. Howe, C.L. and W.C. Mobley, *Long-distance retrograde neurotrophic signaling.* Curr Opin Neurobiol, 2005. **15**(1): p. 40-8.
32. Mousavi, K. and B.J. Jasmin, *BDNF is expressed in skeletal muscle satellite cells and inhibits myogenic differentiation.* J Neurosci, 2006. **26**(21): p. 5739-49.
33. Mousavi, K., D.J. Parry, and B.J. Jasmin, *BDNF rescues myosin heavy chain IIB muscle fibers after neonatal nerve injury.* Am J Physiol Cell Physiol, 2004. **287**(1): p. C22-9.
34. Mousavi, K., W. Miranda, and D.J. Parry, *Neurotrophic factors enhance the survival of muscle fibers in EDL, but not SOL, after neonatal nerve injury.* Am J Physiol Cell Physiol, 2002. **283**(3): p. C950-9.
35. McGuinness, S.L. and R.K. Shepherd, *Exogenous BDNF rescues rat spiral ganglion neurons in vivo.* Otol Neurotol, 2005. **26**(5): p. 1064-72.
36. Fargo, K.N., et al., *Neuroprotective actions of androgens on motoneurons.* Front Neuroendocrinol, 2009. **30**(2): p. 130-41.
37. Yang, L.Y. and A.P. Arnold, *Interaction of BDNF and testosterone in the regulation of adult perineal motoneurons.* J Neurobiol, 2000. **44**(3): p. 308-19.

38. Al-Shamma, H.A. and A.P. Arnold, *Brain-derived neurotrophic factor regulates expression of androgen receptors in perineal motoneurons.* Proc Natl Acad Sci U S A, 1997. **94**(4): p. 1521-6.
39. Yang, L.Y., T. Verhovshek, and D.R. Sengelaub, *Brain-derived neurotrophic factor and androgen interact in the maintenance of dendritic morphology in a sexually dimorphic rat spinal nucleus.* Endocrinology, 2004. **145**(1): p. 161-8.
40. Verhovshek, T. and D.R. Sengelaub, *Trophic effects of brain-derived neurotrophic factor blockade in an androgen-sensitive neuromuscular system.* Endocrinology, 2010. **151**(11): p. 5337-48.
41. Verhovshek, T., et al., *Androgen regulates brain-derived neurotrophic factor in spinal motoneurons and their target musculature.* Endocrinology, 2010. **151**(1): p. 253-61.
42. Dupont-Versteegden, E.E., et al., *Exercise-induced gene expression in soleus muscle is dependent on time after spinal cord injury in rats.* Muscle Nerve, 2004. **29**(1): p. 73-81.
43. Hutchinson, K.J., et al., *Three exercise paradigms differentially improve sensory recovery after spinal cord contusion in rats.* Brain, 2004. **127**(Pt 6): p. 1403-14.
44. Zheng, J., et al., *Clathrin-dependent endocytosis is required for TrkB-dependent Akt-mediated neuronal protection and dendritic growth.* J Biol Chem, 2008. **283**(19): p. 13280-8.
45. Yoshii, A. and M. Constantine-Paton, *BDNF induces transport of PSD-95 to dendrites through PI3K-AKT signaling after NMDA receptor activation.* Nat Neurosci, 2007. **10**(6): p. 702-11.
46. Brunet, A., S.R. Datta, and M.E. Greenberg, *Transcription-dependent and -independent control of neuronal survival by the PI3K-Akt signaling pathway.* Curr Opin Neurobiol, 2001. **11**(3): p. 297-305.
47. Lu, J., et al., *SMAD pathway mediation of BDNF and TGF beta 2 regulation of proliferation and differentiation of hippocampal granule neurons.* Development, 2005. **132**(14): p. 3231-42.
48. Almeida, R.D., et al., *Neuroprotection by BDNF against glutamate-induced apoptotic cell death is mediated by ERK and PI3-kinase pathways.* Cell Death Differ, 2005. **12**(10): p. 1329-43.
49. Chiaruttini, C., et al., *BDNF mRNA splice variants display activity-dependent targeting to distinct hippocampal laminae.* Mol Cell Neurosci, 2008. **37**(1): p. 11-9.
50. Pattabiraman, P.P., et al., *Neuronal activity regulates the developmental expression and subcellular localization of cortical BDNF mRNA isoforms in vivo.* Mol Cell Neurosci, 2005. **28**(3): p. 556-70.
51. Metsis, M., et al., *Differential usage of multiple brain-derived neurotrophic factor promoters in the rat brain following neuronal activation.* Proc Natl Acad Sci U S A, 1993. **90**(19): p. 8802-6.
52. Timmusk, T., et al., *Multiple promoters direct tissue-specific expression of the rat BDNF gene.* Neuron, 1993. **10**(3): p. 475-89.
53. Aid, T., et al., *Mouse and rat BDNF gene structure and expression revisited.* J Neurosci Res, 2007. **85**(3): p. 525-35.
54. Schecterson, L.C. and M. Bothwell, *Novel roles for neurotrophins are suggested by BDNF and NT-3 mRNA expression in developing neurons.* Neuron, 1992. **9**(3): p. 449-63.

55. Ferris, L.T., J.S. Williams, and C.L. Shen, *The effect of acute exercise on serum brain-derived neurotrophic factor levels and cognitive function.* Med Sci Sports Exerc, 2007. **39**(4): p. 728-34.
56. Gold, S.M., et al., *Basal serum levels and reactivity of nerve growth factor and brain-derived neurotrophic factor to standardized acute exercise in multiple sclerosis and controls.* J Neuroimmunol, 2003. **138**(1-2): p. 99-105.
57. Matthews, V.B., et al., *Brain-derived neurotrophic factor is produced by skeletal muscle cells in response to contraction and enhances fat oxidation via activation of AMP-activated protein kinase.* Diabetologia, 2009. **52**(7): p. 1409-18.
58. Gomez-Pinilla, F., et al., *Differential regulation by exercise of BDNF and NT-3 in rat spinal cord and skeletal muscle.* Eur J Neurosci, 2001. **13**(6): p. 1078-84.
59. Gomez-Pinilla, F., et al., *Voluntary exercise induces a BDNF-mediated mechanism that promotes neuroplasticity.* J Neurophysiol, 2002. **88**(5): p. 2187-95.
60. Gonzalez, M., et al., *Disruption of Trkb-mediated signaling induces disassembly of postsynaptic receptor clusters at neuromuscular junctions.* Neuron, 1999. **24**(3): p. 567-83.
61. Lewin, G.R. and Y.A. Barde, *Physiology of the neurotrophins.* Annu Rev Neurosci, 1996. **19**: p. 289-317.
62. Roux, S., et al., *Brain-derived neurotrophic factor facilitates in vivo internalization of tetanus neurotoxin C-terminal fragment fusion proteins in mature mouse motor nerve terminals.* Eur J Neurosci, 2006. **24**(6): p. 1546-54.
63. Altar, C.A., et al., *Anterograde transport of brain-derived neurotrophic factor and its role in the brain.* Nature, 1997. **389**(6653): p. 856-60.
64. Arimura, N., et al., *Anterograde transport of TrkB in axons is mediated by direct interaction with Slp1 and Rab27.* Dev Cell, 2009. **16**(5): p. 675-86.
65. Hirokawa, N., *Kinesin and dynein superfamily proteins and the mechanism of organelle transport.* Science, 1998. **279**(5350): p. 519-26.
66. Lemmon, M.A. and J. Schlessinger, *Cell signaling by receptor tyrosine kinases.* Cell, 2010. **141**(7): p. 1117-34.
67. Sorkin, A. and M. von Zastrow, *Endocytosis and signalling: intertwining molecular networks.* Nat Rev Mol Cell Biol, 2009. **10**(9): p. 609-22.
68. Zweifel, L.S., R. Kuruvilla, and D.D. Ginty, *Functions and mechanisms of retrograde neurotrophin signalling.* Nat Rev Neurosci, 2005. **6**(8): p. 615-25.
69. Friedman, B., et al., *BDNF and NT-4/5 exert neurotrophic influences on injured adult spinal motor neurons.* J Neurosci, 1995. **15**(2): p. 1044-56.
70. Henderson, C.E., et al., *Neurotrophins promote motor neuron survival and are present in embryonic limb bud.* Nature, 1993. **363**(6426): p. 266-70.
71. Mitsumoto, H., et al., *Arrest of motor neuron disease in wobbler mice cotreated with CNTF and BDNF.* Science, 1994. **265**(5175): p. 1107-10.
72. Pasinelli, P. and R.H. Brown, *Molecular biology of amyotrophic lateral sclerosis: insights from genetics.* Nat Rev Neurosci, 2006. **7**(9): p. 710-23.
73. Gonzalez de Aguilar, J.L., et al., *Amyotrophic lateral sclerosis: all roads lead to Rome.* J Neurochem, 2007. **101**(5): p. 1153-60.
74. Wijesekera, L.C. and P.N. Leigh, *Amyotrophic lateral sclerosis.* Orphanet J Rare Dis, 2009. **4**: p. 3.

75. Bach, J.R., *Amyotrophic lateral sclerosis: prolongation of life by noninvasive respiratory AIDS.* Chest, 2002. **122**(1): p. 92-8.
76. Lyall, R.A., et al., *Respiratory muscle strength and ventilatory failure in amyotrophic lateral sclerosis.* Brain, 2001. **124**(Pt 10): p. 2000-13.
77. Okamoto, K., et al., *Axonal swellings in the corticospinal tracts in amyotrophic lateral sclerosis.* Acta Neuropathol, 1990. **80**(2): p. 222-6.
78. Sasaki, S. and M. Iwata, *Ultrastructural study of synapses in the anterior horn neurons of patients with amyotrophic lateral sclerosis.* Neurosci Lett, 1996. **204**(1-2): p. 53-6.
79. Appel, S.H., *A unifying hypothesis for the cause of amyotrophic lateral sclerosis, parkinsonism, and Alzheimer disease.* Ann Neurol, 1981. **10**(6): p. 499-505.
80. Xiong, H., et al., *Neurotrophins induce BDNF expression through the glutamate receptor pathway in neocortical neurons.* Neuropharmacology, 2002. **42**(7): p. 903-12.
81. Sasaki, S. and M. Iwata, *Ultrastructural change of synapses of Betz cells in patients with amyotrophic lateral sclerosis.* Neurosci Lett, 1999. **268**(1): p. 29-32.
82. Sasaki, S. and M. Iwata, *Dendritic synapses of anterior horn neurons in amyotrophic lateral sclerosis: an ultrastructural study.* Acta Neuropathol, 1996. **91**(3): p. 278-83.
83. Kalb, R.G., *Regulation of motor neuron dendrite growth by NMDA receptor activation.* Development, 1994. **120**(11): p. 3063-71.